1965

The effect of selected impurities on some optical properties of silicon

Neil Herman Schilmoeller
Iowa State University

THE EFFECT OF SELECTED IMPURITIES ON SOME OPTICAL PROPERTIES OF SILICON

by

Neil Herman Schilmoeller

A Dissertation Submitted to the
Graduate Faculty in Partial Fulfillment of
The Requirements for the Degree of
DOCTOR OF PHILOSOPHY

Major Subjects: Mechanical Engineering
Nuclear Engineering

Approved:

Signature was redacted for privacy.

In Charge of Major Work

Signature was redacted for privacy.

Heads of Major Departments

Signature was redacted for privacy.

Dean of Graduate College

Iowa State University
Of Science and Technology
Ames, Iowa

1965

TABLE OF CONTENTS

NOMENCLATURE

n	index of refraction
κ	index of absorption
E_y	electric wave amplitude, volts/centimeter
χ	distance, centimeters
t	time, seconds
A	electric wave maximum amplitude, volts/centimeters
λ	wavelength, centimeters
ω	angular frequency, radians/second
c	velocity of light
r_λ	monochromatic reflectance
ρ	specific resistivity, ohm centimeters
u	frequency ratio
υ	frequency, cycles/second
δ	frequency, cycles/second
λ_o	wavelength constant, centimeters
m	mass, grams
f_o	oscillator strength, dynes/centimeter
e	electronic charge, electrostatic unit
λ_r	wavelength constant
σ	conductivity, $(\text{ohm cm})^{-1}$
ε	emissivity
R_s	specular reflection
R_o	specular reflection for smooth surface
b	root mean square surface level, centimeters

$\Delta\theta$	solid angle, steradians
T_o	degeneracy temperature, degrees Kelvin
h	Planck's constant, erg second
n_d	impurity concentration, atoms/cubic centimeter
$\underline{k}$	Boltzmann's constant, electron volts per degree Kelvin
k	absorption coefficient, cm^{-1}
v	velocity, centimeters/second
α	dielectric constant, charge·centimeters/volt
τ	relaxation time, seconds
E_χ	electric field, volts/centimeter
γ	damping coefficient, $(seconds)^{-1}$
ω_o	natural frequency, radians/second
n*	complex index of refraction
α*	complex dielectric constant
a_λ	monochromatic absorptance
t_λ	monochromatic transmittance
E_g	forbidden gap energy, electron volts
$\bar{k}_i$	initial wave number, $(centimeters)^{-1}$
$\bar{q}_i$	photon wave number, $(centimeters)^{-1}$
$\bar{k}_f$	final wave number, $(centimeters)^{-1}$
E'	indirect but minimum gap energy, electron volts
E_i	donor energy level, electron volts
E_f	Fermi energy level, electron volts
E_c	conduction band edge energy, electron volts
E_v	valance band edge energy, electron volts
r_{ref}	reflectance of reference surface

NOMENCLATURE

n	index of refraction
κ	index of absorption
E_y	electric wave amplitude, volts/centimeter
χ	distance, centimeters
t	time, seconds
A	electric wave maximum amplitude, volts/centimeters
λ	wavelength, centimeters
ω	angular frequency, radians/second
c	velocity of light
r_λ	monochromatic reflectance
ρ	specific resistivity, ohm centimeters
u	frequency ratio
υ	frequency, cycles/second
δ	frequency, cycles/second
λ_o	wavelength constant, centimeters
m	mass, grams
f_o	oscillator strength, dynes/centimeter
e	electronic charge, electrostatic unit
λ_r	wavelength constant
σ	conductivity, $(\text{ohm cm})^{-1}$
ε	emissivity
R_s	specular reflection
R_o	specular reflection for smooth surface
b	root mean square surface level, centimeters

$\Delta\theta$	solid angle, steradians
T_o	degeneracy temperature, degrees Kelvin
h	Planck's constant, erg second
n_d	impurity concentration, atoms/cubic centimeter
$\underline{k}$	Boltzmann's constant, electron volts per degree Kelvin
k	absorption coefficient, cm^{-1}
v	velocity, centimeters/second
α	dielectric constant, charge·centimeters/volt
τ	relaxation time, seconds
E_χ	electric field, volts/centimeter
γ	damping coefficient, $(seconds)^{-1}$
ω_o	natural frequency, radians/second
n*	complex index of refraction
α*	complex dielectric constant
a_λ	monochromatic absorptance
t_λ	monochromatic transmittance
E_g	forbidden gap energy, electron volts
$\bar{k}_i$	initial wave number, $(centimeters)^{-1}$
$\bar{q}_i$	photon wave number, $(centimeters)^{-1}$
$\bar{k}_f$	final wave number, $(centimeters)^{-1}$
E'	indirect but minimum gap energy, electron volts
E_i	donor energy level, electron volts
E_f	Fermi energy level, electron volts
E_c	conduction band edge energy, electron volts
E_v	valance band edge energy, electron volts
r_{ref}	reflectance of reference surface

E_{ref}	energy reflected from reference surface, ergs
E_o	energy incident on reference surface, ergs
r_{sam}	reflectance of specimen surface
ev	electron volts

I. INTRODUCTION

There has been a good deal of interest recently in the study of the optical properties of semiconductors because of their behavior both as a metal and as a dielectric. The optical properties of these semi-metals or semiconductors vary with the material, with the structure and with the impurity.

Pearson and Bardeen (32) have shown that small amounts of specific impurities in silicon and germanium drastically affect the electrical properties of these solids. Fan and Becker (13) have shown that the infrared absorption characteristics of these same materials are also affected by the addition of specific impurities.

For this study the transmission, total reflection and diffuse reflection were measured as a function of the wave length and from these data the index of refraction and the absorption coefficient were calculated. Each of the measured quantities was observed over a range of impurity concentrations.

This study resulted from an examination of a method for determining the absorption edge of a semiconductor by measurement of the diffusely reflected radiation, proposed by Fochs (14). Fochs suggested that a study of the effect of impurity concentrations on the measurement of the absorption edge and on the diffuse reflectance by his method would be quite interesting and informative. This study was initiated, in part, to

determine this effect for one material, silicon, with two specific impurities, boron and phosphorus. The effect of these impurities on other optical properties was also studied.

II. LITERATURE SURVEY

The intensive study of the optical properties of materials had its beginnings about 1870 with the derivation of Maxwell's field equations (27). Although the study of optics began much earlier, the study of physical optics required knowledge of the microstructure of matter and some feeling about how the atoms in a solid might behave in the changing electric field of electromagnetic radiation.

The theory of the propagation of electromagnetic waves through materials is based on Maxwell's field equations. With this theory one can explain the reflection of electromagnetic radiation from an interface between two media in terms of the index of refraction, n, and the index of absorption, κ. These two quantities are contained in the following equation appearing in an article by Snyder (37).

$$E_y(\chi,t) = A\, e^{\frac{4\pi\kappa\chi}{\lambda}}\, e^{i\omega(t - \frac{n\chi}{c})} \qquad [1]$$

E_y - Electric field component polarized in the y direction

ω - Frequency of radiation

κ - Index of absorption

c - Velocity of light in free space

n - Index of refraction

t - Time

χ - distance

The two quantities, n and κ, are dependent on the frequency of the incident radiation (42). Metals, for example, have high reflectances in the infrared region where the index of absorption and index of refraction are constant. As the wavelength gets shorter the electrons within the metal cannot follow the higher frequency vibrational electric wave. The materials then become more transparent as the absorption within the lattice structure drops (19). Snyder (37) suggests that the action of resistive forces on the electronic vibration causes the reflectivity, absorption and transmission to vary at longer wavelengths, that is at lower frequencies. This variation in the optical properties of reflectivity and absorption also appears in the index of refraction and the index of absorption (7).

Use of Maxwell's field equations to treat the interaction of radiation with materials was the macroscopic approach to the problem of the determination of the optical constants. Drude (12) and Lorentz (25) were the first to present the microscopic approach. They assumed the material in question was made up of a series of harmonic oscillators. By applying the theory of energy absorption by such oscillators the absorption and reflection were calculated as a function of the frequency of the driving force and of the number of oscillators present in the material. Hagen and Rubens (18), using the theory set down by Drude and Lorentz, were quite successful

in calculating the dependence of infrared region reflectance of metals on the wavelength of the radiation and on the electrical resistivity. Their equation was as follows,

$$r_\lambda = 1 - 36.05 \sqrt{\frac{\rho}{\lambda}} \qquad [2]$$

ρ - specific resistivity, ohm cm

λ - wavelength, microns

Another microscopic approach was derived by Kronig (23) who used quantum mechanics to treat the periodic potential model of a metallic conductor. From this approach Kronig was able to derive an equation for reflectance.

$$r_\lambda = 1 - 36.05 \sqrt{\frac{\rho}{\lambda}} \sqrt{\sqrt{u^2 + 1} - u} \qquad [3]$$

$u = \frac{\upsilon}{\delta}$ a ratio of frequencies

υ - frequency of the incident radiation

δ - half breadth of the absorption peak at the vicinity of the main absorption peak

For the case of small u, i.e. infrared and longer wavelengths (25), this equation reduces to the Hagen-Rubens equation.

Price (34) using Kronig's basic approach developed a more useful form of the original equations for reflection from a

metallic conductor. These equations correctly predicted the variation of reflectivity with wavelength for several metals in the infrared region, beyond 2 microns (6). This theoretical approach failed to explain the rapid drop in reflectivity in the visible region which is observed for most metals (16).

The quantum mechanical approach of Price (34) indicates 3 basic regions. For very short wavelengths, up to 0.1 micron, the reflectance is predicted to be proportional to the fourth power of the wavelength.

$$r_\lambda = \frac{1}{16}\left(\frac{\lambda}{\lambda_o}\right)^4 \qquad [4]$$

$$\lambda_o = \frac{\pi m c^2}{f_o e^2}$$

f_o - oscillator strength

c - velocity of light

e - electronic charge

For long wavelengths the Hagen-Rubens equation is obtained. In the intermediate range, between 0.1 and 0.4 microns, the reflectivity is a constant

$$r = 1 - 2\frac{\lambda_r}{\lambda_o}$$

$$\lambda_r = \frac{c}{2\sigma} \qquad [5]$$

Figure 1 shows the variation of $\frac{\varepsilon^2}{4r}$ against the logarithm of the wavelength for an ideal metal. ε is the emissivity of the material. The three main spectral regions indicated by the three equations above are shown.

A somewhat different type of study using specular and diffuse reflectance was undertaken by Bennett and Porteus (4). Using a theoretical treatment for reflection of microwaves from rough water, these experimenters tried to apply the theory to radiant energy in the visible region. The light was reflected from ground stainless steel or glass plates which were coated with an evaporated film of aluminum. Various surface textures were used to determine their effect on the specular and diffuse reflectance.

This study relates the root-mean-square height of the surface irregularities and the wavelength to the specular reflectivity. The following equation was the result of this study for wavelengths much greater than b.

$$R_s = R_o \exp[-4\pi\frac{\gamma^2}{\lambda^2}] \qquad [6]$$

R_s - Specular reflection

R_o - Specular reflection from a perfectly smooth surface

b - Root-mean-square deviation of the surface from a mean level

λ - Wavelength in microns

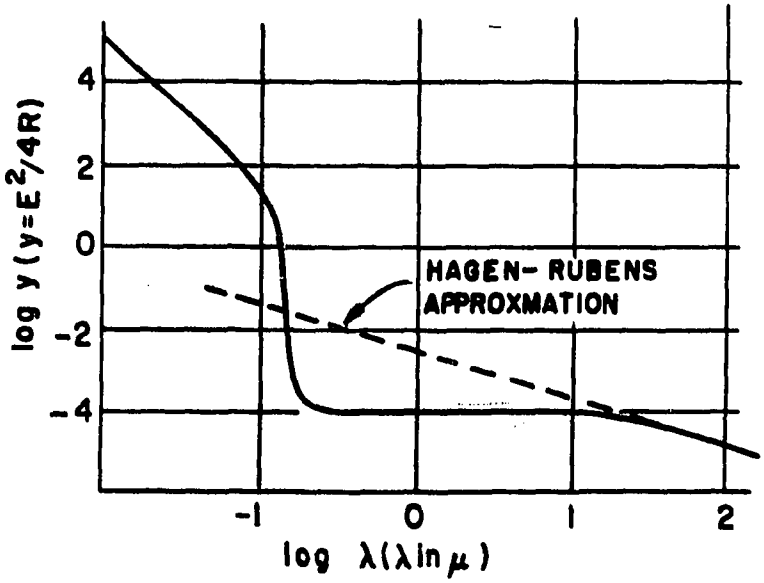

Figure 1. The variation of $E^2/4R$ with wavelength for an ideal metal (6)

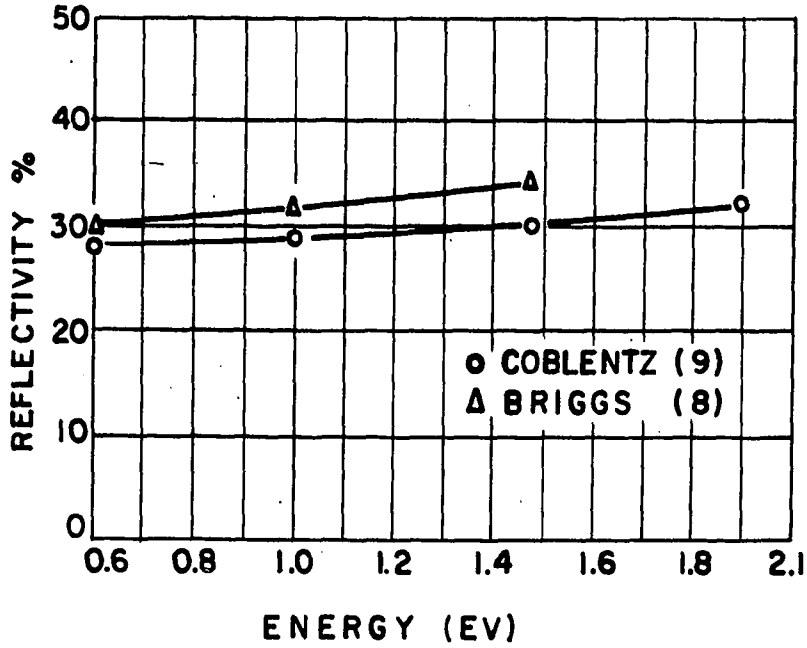

Figure 2. Reflectivity for silicon

When the wavelengths are of the order of b, the diffuse component becomes important and is accounted for by the second term in the following equation

$$R_s = R_o \exp[-4\pi\frac{\sigma^2}{\lambda^2}] + R_o \frac{2^5\pi^4}{m^2} (\frac{\sigma}{\lambda})^4 (\Delta\theta)^2 \qquad [7]$$

m - Root mean square slope of the profile of the surface

$\Delta\theta$ - Is the solid angle intercepted by the recording instrument

Bennett and Porteus formulas above give a technique for measuring the surface roughness by measuring the specular and diffuse reflectivity. This study does not discuss the volume properties and considers the surface a perfect conductor, due to the aluminun surface coating.

Studies of reflectivity of polycrystalline silicon and germanium were conducted by Coblentz (9) about 1911. He measured the reflectivity of polished silicon up to about 10 microns. Figure 2 shows his results. Nothing is known of the electrical or other properties of his specimens.

Following the development of quantum mechanics it became possible to obtain a greater insight into the nature of materials. It is now known that the electrical properties of semiconductors are greatly affected by small amounts of impurities, too small to be detected by ordinary methods.

Brattain and Briggs (7) have provided some data on the

infrared properties of germanium which show how some optical properties vary with temperature. Fan and Becker (13) presented a detailed paper in which they present the infrared optical properties of a few specimens of silicon and germanium. The properties examined were reflectance, transmission and absorption where significant variations were noted at wavelengths above 1 micron. Pearson and Bardeen (32) examined the electrical properties of polycrystalline silicon doped with concentrations of boron and phosphorus. Using impurity concentrations ranging from 10^{17} to 10^{21} atoms per cubic centimeter, the electrical properties of conductivity and Hall coefficient showed drastic changes both with temperature and with concentration. However, beyond a concentration of impurity atoms of about 10^{19} atoms per cubic centimeter the property variations with temperature nearly ceased. The onset of this condition is also temperature dependent as will be shown later. This was attributed to the degeneracy of the energy levels in the electron gas in the lattice to a continuum of energy levels (32). That is, the temperature no longer plays an important role in determining the number of charge carriers available. An equation is given by Pearson and Bardeen (32) relating the onset of the degenerate condition with temperature and the number of impurity atoms,

$$T_o = \left(\frac{h^2}{8km}\right)\left(\frac{3}{\pi}\right)^{2/3} n^{2/3} \qquad [8]$$

where

T_o - Temperature at which degeneracy begins

h - Planck's constant

k - Boltzmann's constant

m - Electron mass

n - Number of charge carriers

Morin and Maita (28) studied the electrical properties of single crystal silicon doped with arsenic and boron and noted this degeneracy effect for impurity concentrations of about 10^{18} to 10^{19} atoms per cubic centimeter.

Most of the reflectance studies to date have been concerned with total reflectivity. Reflectivity from the specimen is most often compared to an evaporated aluminum mirror. Lark-Horovitz and Meissner (24) used this method for reflective data from 1 to 10 microns for silicon. No transmission data is supplied for these specimens.

Using another method Fochs (14) found that the diffuse reflection spectrum of a powdered semiconductor is characterized by an increase in the diffuse reflectivity as the individual particles become relatively transparent. The diffuse reflectance was measured by placing a 1 to 2 millimeter thick sample of a powdered specimen at the focal point of the concave collecting mirror. The monochromatic radiation was directed through the center of the mirror at the specimen. The reflected energy, collected by the mirror was directed

toward a photocell or lead sulfide detector. Thus, about 25 percent of the diffusely reflected energy was collected (14).

Fochs indicates that the exponential drop in the absorption coefficient causes a definite linear range in the region of the largest slope of the reflectance versus wavelength curve. The extension of this linear range to zero reflectance is suggested as a more universal method to determine the absorption edge. The absorption edge corresponds to the energy at which electrons can just begin to cross the forbidden energy band. Wooley and Warner (43) used this method to determine the absorption edges of some Group III to Group IV compounds.

Moss (29) has discussed in detail the optical properties of semiconductors. He reviews the work on silicon and germanium as well as on several other materials. This book also includes some theoretical discussions of the problems of relating the optical properties to the microscopic and macroscopic properties of the solid. A more recent article by Stern (38) discusses the quantum mechanical considerations of formulating the electromagnetic interaction problem for metals and dielectrics and indicates that much study of this area is needed.

It has been noted in this literature survey that small amounts of specific impurities affect the optical and electrical properties of semiconductors. Fochs (14) indicated in his paper on the determination of the absorption edge using

diffuse reflectance that the effects of impurity concentrations were not known. Pearson and Bardeen (32) reported that degeneracy can set in at certain temperature ranges and/or at high impurity concentrations. It was, therefore, decided to investigate the effects of some special impurities on the optical properties, reflectance, absorption coefficient and index of refraction of silicon, with particular attention to the diffuse reflectance.

III. THEORETICAL CONSIDERATIONS

The basis for a theoretical discussion of the optical properties of materials can be divided into two categories. In the first category is the problem of relating the reflectance of electromagnetic radiation to measurable macroscopic properties of a specimen. The macroscopic properties are usually the absorption coefficient and the index of refraction. In the second category the microscopic approach is used to relate the macroscopic properties of a specimen to the behavior of the individual electrons, atoms or other particles in the specimen.

Some highlights from these two areas will be presented in the following pages along with a discussion of some solid state considerations for semiconductors. This last area on semiconductors was included since the material studied for this thesis was a semiconductor. The purpose of this discussion is to indicate some possible theoretical approaches which will help to explain the interaction of electromagnetic radiation with certain solid materials. This basis will then be used to indicate some possible reasons why the optical properties of these solids vary with wavelength and with temperature.

A. Electromagnetic

The theory of the propagation of electromagnetic waves in conducting materials is based on Maxwell's field equations.

If we use this theory, an equation can be developed relating the reflectivity to the macroscopic properties, the index of refraction and the index of absorption (29). The indices of absorption and refraction can be related to the electrical conductivity and the wavelength of the incident radiation.

As a result of the solution for Maxwell's equations for a wave advancing along the χ axis and incident on a material, it can be shown (37) that the following expression for reflectivity results,

$$r_\lambda = \frac{(n-1)^2 + \kappa^2}{(n+1)^2 + \kappa^2} \qquad [9]$$

where

r_λ - Monochromatic reflectivity

n - Index of refraction

κ - Index of absorption

n represents the ratio of c, the velocity of the light wave in empty space (or in air, approximately) with respect to v, its velocity within the medium. In passing a distance χ through an absorbing medium the energy, or amplitude of the wave is reduced by the factor $e^{-k\chi}$. The energy of a wave is proportional to the square of its amplitude so the amplitude is reduced by $e^{-2k\chi}$. For this discussion it is preferable to use the index of absorption, κ, which is related to k as follows,

$$k = \frac{4\pi\kappa}{\lambda} \qquad [10]$$

Examination of equation 9 shows that when κ is large compared to n, r approaches one. In other words radiant energy at a particular wavelength, which is strongly absorbed internally, is strongly reflected. This is the reason the colors of such a medium by transmission and reflection are complementary, for example, a thin film of gold metal appears blue by the transmitted light. $\kappa = 0$ gives,

$$r_\lambda = \frac{(n-1)^2}{(n+1)^2} \qquad [11]$$

which is Snell's law for reflectivity at normal incidence.

If we use another approach, the indices of refraction and absorption can be expressed in terms of the dielectric constant, α, the conductivity, σ, and the relaxation time, τ, as outlined by Snyder (37). For the case where the permeability equals one, Snyder obtained the following equations.

$$n = \sqrt{\frac{1}{2}\sqrt{\alpha^2 + 4\sigma^2\tau^2} + \alpha}$$

$$\kappa = \sqrt{\frac{1}{2}\sqrt{\alpha^2 + 4\sigma^2\tau^2} - \alpha}$$

From these equations we get,

$$n^2 + \kappa^2 = \sqrt{\alpha^2 + 4\sigma^2\tau^2}$$

Then on substitution into equation 9 the reflectivity becomes,

$$r_\lambda = \frac{\sqrt{4\sigma^2\tau^2 + \alpha^2} + 1 - \sqrt{2\left(\sqrt{4\sigma^2\tau^2 + \alpha^2} + \alpha\right)}}{\sqrt{4\sigma^2\tau^2 + \alpha^2} + 1 + \sqrt{2\left(\sqrt{4\sigma^2\tau^2 + \alpha^2} + \alpha\right)}}$$

For $\alpha << \sigma\tau$, this can be expressed as

$$r_\lambda = \frac{2\tau\sigma - 2(\tau\sigma)^{1/2} + 1}{2\tau\sigma + 2(\tau\sigma)^{1/2} + 1} \qquad [12]$$

Harrison (19) shows that if $\sigma\tau >> 1$, equation 12 can be expanded in a power series.

$$r_\lambda = 1 - 2(\tau\sigma)^{-1/2} + 2(\tau\sigma)^{-1} - (\tau\sigma)^{-3/2} \qquad [13]$$

As a first approximation Hagen and Rubens (18) used the first two terms to calculate the reflectivity for metallic conductors. The results from this equation are plotted as a dotted line in Figure 1. For wavelengths longer than 10^μ this equation approximates the reflectivity of several metals (18).

The Hagen-Rubens equation does not give the correct values for reflectivity for semiconductors in the infrared region of the spectrum due to the greatly reduced conductivities (29). In the optical region this equation does not apply to either a metal or a semiconductor. If we use suitable assumptions, expressions for n and κ can be derived which provide the correct answers for the very limited case of metallic conductors in the infrared spectrum. To provide better results more understanding of the microscopic behavior of materials is needed.

B. Dispersion

The electric field of a wave passing through a medium produces forced vibrations of the electrically charged particles. Several types of such particles may be present within a given substance, bound electrons, free electrons and ions. Their composite effect determines the total change in the optical properties of the system.

The vibrational characteristics of the particles may vary widely from one frequency to another. These characteristics and the concentration of the particles to which they belong fix the values of the dielectric constant, α, index of refraction, n, and the absorption coefficient, k at a given wavelength. The behavior of a single particle may be analyzed on the basis of the classical electron theory of matter (11). This analysis accounts qualitatively for the phenomena of reflection and absorption.

The electron theory assumes that matter is composed of positively and negatively charged particles elastically bound together by their mutual attraction. An electric field, E_χ, displaces the charged particles from the equilibrium position in the direction of the χ axis. The restoring force is assumed to vary linearly with the displacement, χ. All motions of the bound particle are assumed to be resisted by a viscous damping force which is linearly proportional to the velocity of the particle. This discussion is therefore based on the classical model of the harmonic oscillator. The bound particle has mass, m, and charge, e, and is in an alternating field, $Ae^{i\omega t}$. The equation of motion is as follows,

$$m\frac{d^2\chi}{dt^2} + m\gamma\frac{d\chi}{dt} + m\omega_o{}^2\chi = eAe^{i\omega t} \qquad [13]$$

where ω_o is the natural frequency of the particle and equals $(\frac{f}{m})^{1/2}$, where f is the restoring force constant. γ is the damping coefficient. This second term results from the fact that classically a charged particle emits radiation when it is accelerated. Dekker (11) gives the solution to this equation for forced damped vibration as

$$\chi(t) = \frac{e}{m} \cdot \frac{E_o e^{i\omega t}}{\omega_o{}^2 - \omega^2 + i\gamma\omega} \qquad [14]$$

For an electron Dekker gives a natural frequency of about 10^{15}

per second while for an ion it is about 10^{13} per second, corresponding to the infrared portion of the spectrum. Dekker shows how the dielectric constant varies with frequency as a result of the periodic damped displacement of the charged particle. As the system nears the natural frequency energy is absorbed from the incident beam. With this change in absorption the reflection and transmission vary also.

The complex index of refraction is usually related to the dielectric constant for optical work. Maxwell's equations for a non-magnetic insulator give an expression for the velocity of propagation of light as follows,

$$v = \frac{c}{\sqrt{\alpha}}$$

Since the index of refraction, n, is defined as $\frac{c}{v}$, the Maxwell relation, $\alpha = n^2$, follows. If absorption takes place the component of the light wave polarized in the y direction and propagating in the χ direction can be written as follows,

$$E_y(\chi,t) = Ae^{-\omega\kappa\chi/c}\, e^{i\omega(t-n\chi/c)} \qquad [15]$$

Now instead of this equation one can write,

$$E_y(\chi,t) = Ae^{i\omega(t-n^*\chi/c)} \qquad [16]$$

where n* is the complex index of refraction and must equal

$n - i\kappa$. From this relation for n^* and Maxwell's relation of $(n^*)^2 = \alpha^*$ we get,

$$\alpha' = n^2 - \kappa^2 \quad \text{and} \quad \alpha'' = 2n\kappa$$

Thus the index of refraction and index of absorption are related to the dielectric constant for an absorbing medium. The dielectric constant, in turn, is related to the displacement of the charged particle so that n and κ are related to the behavior of the individual oscillator driven by the light wave. Harrison (19) calculates the reflectivity using the results from disperision theory for free electrons, bound electrons and combinations of these two. With this he was able to indicate the effect of the bound electron on the variation of reflectivity as a function of wavelength for a model metal. The effect observed was quite similar to those observed experimentally for copper and other metals at ultraviolet wavelengths (19).

The dispersion theory outlined here gives a possible basis for some of the irregularity in reflectivity and absorption for some solids. The important idea is the concept of the effects of the bound and free electron on the optical properties of solids.

C. Relation Between Reflection, Absorption and Transmission

When radiant energy impinges on a surface, part of it is reflected and part is absorbed. This absorbed radiant energy

is converted to thermal energy which tends to raise the temperature of the body. If the body is not opaque, a portion of the incident energy passes through. The sum of the energy absorbed, reflected and transmitted equals the incident energy.

Most metals are opaque to visible and infrared radiation, whereas many dielectric substances are more or less transparent in some regions of the spectrum and opaque in others. Semiconductors are between these two, behaving as dielectrics for some wavelengths and temperatures, and as metals at other wavelengths and temperatures.

For any material over a small wavelength interval centered around wavelength λ, the following relation between the spectral reflectance, spectral absorptance, and spectral transmittance applies.

$$r_\lambda + a_\lambda + t_\lambda = 1 \qquad [17]$$

For opaque bodies t_λ equals 0 and

$$r_\lambda + a_\lambda = 1$$

r_λ - Spectral reflectance

a_λ - Spectral absorptance

t_λ - Spectral transmittance

Each of these quantities is dependent on the absorption characteristics of the medium.

When radiant energy impinges on a surface, the reflected energy at the point of incidence depends on both the material and its surface condition. The radiant energy entering the medium is absorbed along the path of travel to an extent dependent upon the absorptive characteristics of the material and on the length of path of the radiation in the medium. Energy that is not absorbed may reach the opposite face and emerge or be reflected back into the medium. Harrison (19) and Gubareff (17) examine each of these cases in detail. Harrison obtains the following equation relating transmittance, t, reflectance, r, and the absorption coefficient, k, for the case where internal reflections cannot be neglected.

$$t = (1 - r)^2 e^{-\kappa X} [1 + (re^{-\kappa X})^2] \qquad [19]$$

The term $e^{-\kappa X}$ and $(re^{-\kappa X})^2$ in the brackets account for absorption. If the specimen is thick enough to make $e^{-\kappa X}$ substantially equal to zero, the body is opaque. For this case the internal absorption terms disappear and t equals zero.

If multiple reflections inside the medium are neglected, the ratio of the transmitted energy to the incident energy may be written as,

$$t = (1-r)^2 e^{-\kappa X} \qquad [20]$$

Fan and Becker (13) use this equation to evaluate the absorption coefficient for polycrystalline germanium. This equation will be used later to evaluate the absorption coefficient, k, knowing the transmittance and reflectance for the semiconductor used in this study.

D. Semiconductors

As indicated in the section on dispersion theory, absorption by bound and by free electrons are significant in certain materials. For absorption of electromagnetic radiation there are four types of electrons or charge carriers to be considered: (1) inner shell electrons, (2) valence band electrons, (3) free carriers which includes holes and electrons, and (4) electrons bound to localized centers of impurity or other defects.

The first group does not contribute to absorption in the spectral region of this study and will not be considered further. The second group is of great importance in the study of absorption and other fundamental properties of semiconductors. The third group, free carriers, provides a continuous absorption spectrum as in a metal. Harrison (19) and others have treated these metallic materials in great detail. Doped semiconductors display some effects due to nearly free charge carriers, both electrons and holes. Group four electrons are important in the F-center studies for alkali-halides and are treated in the literature (11).

The valence electrons are the most important in semiconductors. In an ideal semiconductor at zero temperature the valence band is completely full, so that an electron cannot be excited to a higher level in the band. The only possible absorption is that of a quantum with enough energy to excite an electron across the forbidden zone into the empty conduction band. In practice this absorption is characterized by a sharp increase in absorption as the energy of the quantum is raised to a level where the transition is possible. Below this level the material is relatively transparent.

If the energy band is plotted in $\bar{k}$ space, $\bar{k}$ equals $\frac{2\pi}{\lambda}$, as shown in Figure 3a, the conduction band minimum and the valence band maximum occur at $\bar{k} = 0$. Absorption may, but not necessarily, occur at $h\upsilon = E_g$, where E_g is the minimum width of the forbidden region.

Quantum mechanical selection rules state that the difference between the final state wave vector, $\bar{k}_f$, and the initial state wave vector, $\bar{k}_i$, must equal the wave vector of the radiation, $\bar{q}$. However, for wavelengths greater than about 1 micron, $\bar{q}$ is very small compared to $\bar{k}$ so that $\bar{k}_f \approx \bar{k}_i$. For these values of $\bar{q}$ the electron can only make transitions to states of higher energy having the same $\bar{k}$ values, that is, vertical transitions only. In practice non-vertical transitions do occur but these transitions are often few in number and therefore of much lower intensity.

For the energy band in Figure 3a then intense absorption

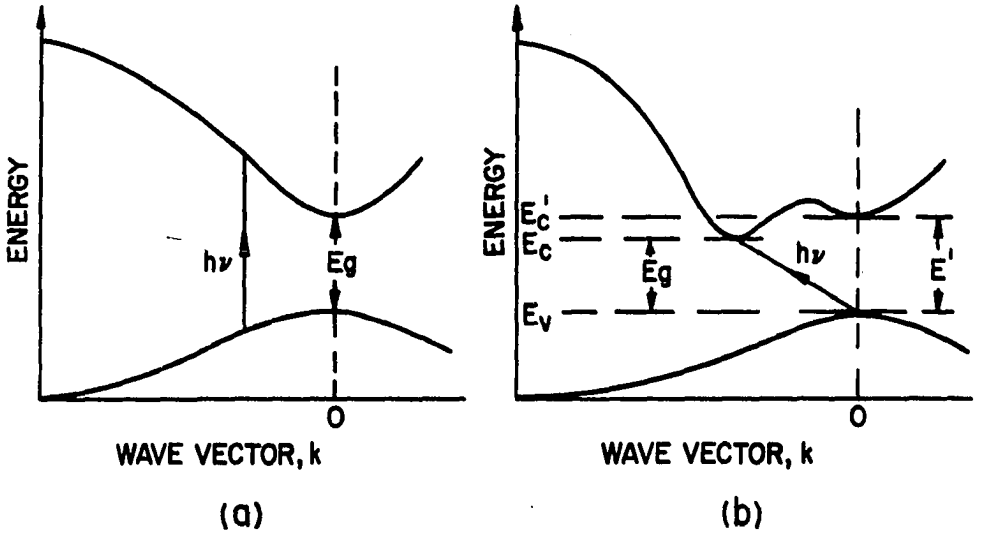

Figure 3. Possible energy bands for semiconductors (29)

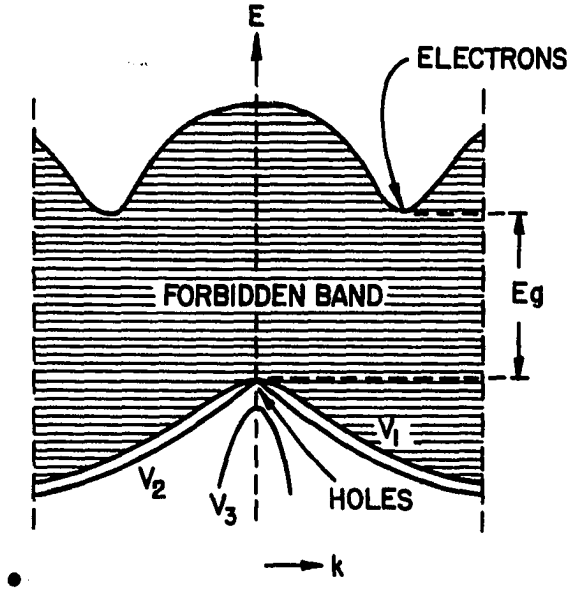

Figure 4. Schematic representation of the energy band structure for silicon along the 100 axis (20)

would occur at energies greater than E_g and cease more or less abruptly at $h\upsilon = E_g$.

Some semiconductors have energy band structures with minimums in the conduction band at other than $\bar{k} = 0$ where the maximum in the valence band occurs, see Figure 3b. Silicon and germanium are two materials in this category, see Figure 4 (21). For these cases intense absorption will cease at wavelength corresponding to the minimum vertical gap, $E' = h\upsilon$. There are always factors present under normal conditions which cause a relaxation of the selection rules and permit some non-vertical transitions. The momentum is conserved in these cases probably by an interaction with a phonon, or lattice vibration, so that absorption will generally continue down to $h\upsilon = E_g$, the energy gap minimum. This can cause the absorption edge to display a tail or transition while varying the energy of the incident quanta from the region of intense absorption to the region of semi-transparency.

In addition to the effects discussed above, certain elements added to silicon, for example, cause a doped effect. The charge carriers can be varied by varying the amount of the doping element and these charge carriers are very lightly bound to the parent atom.

Doped semiconductors can be treated from a simple band model with the impurity levels in the forbidden region. Figure 5 shows this situation for n-type and p-type crystals. For silicon the n-type is obtained by doping with a group V

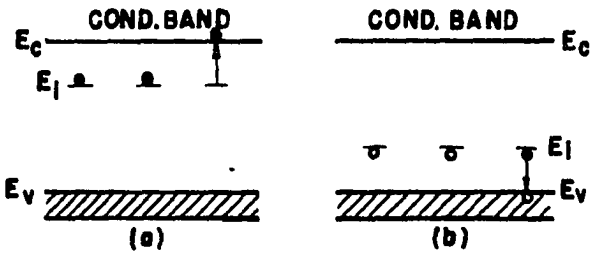

Figure 5. Schematic representation of energy levels of an n-type semiconductor, a, and a p-type, b

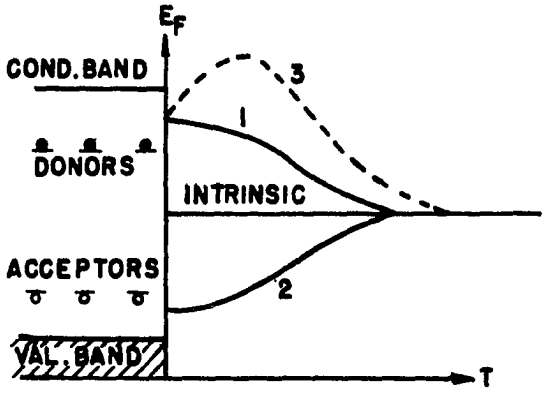

Figure 6. A representation of the variation of Fermi level with temperature for curve 1) insulator with donors, curve 2) insulator with acceptors and curve 3) case where electron gas in conduction band is degenerate over a range of temperatures (11)

element, phosphorus, and the p-type by doping with a group III element, boron.

For an n-type semiconductor, for example, the Fermi level is usually located between the donor level and the conduction band. Dekker (11) gives an expression for the position of the Fermi level for this case as a function of the number of donors, n_d, and the absolute temperature.

$$E_f = \frac{1}{2}[E_i + E_c] + \frac{\underline{k}T}{2} \ln\left[\frac{n_d}{2\left(2\pi m_e^* \frac{\underline{k}T}{h^2}\right)^{3/2}}\right] \qquad [21]$$

$\underline{k}$ - Boltzmann's constant

m_e^* - Effective mass of the electrons

h - Planck's constant

E_i - Donor energy level

E_c - Conduction band edge energy

For $T = 0$, E_f is exactly half way between the donor level and the bottom of the conduction band. Figure 6 shows the change in Fermi level with temperature for a donor level 0.2 ev below the conduction band (11). Curve 1 is for an n-type material, curve 2 for a p-type material and curve 3 for the case in which the electron gas in the conduction band is degenerate over certain temperature ranges.

Due to the small value of $E_v - E$ for silicon--for example, 0.05 electron volts--many of the donors will be

ionized at room temperature and will be available for absorption processes for radiation with wavelengths shorter than approximately 25 microns. After the donors are ionized, the only electrons which can add to the charge carriers must come from the valence band which requires that they absorb at least E_g energy to cross the forbidden region. This region between impurity carriers and intrinsic carriers is called the exhaustion range of temperature. Pearson and Bardeen (32) show this for the case of n-type germanium. As the temperature is raised, the number of charge carriers looks more and more like that for a simple intrinsic specimen.

The number of donor atoms also affect the way the Fermi level moves as the temperature increases from zero degrees. If the number of donors is too large, the Fermi level actually enters the conduction band and the electron gas is said to be degenerate (32). The electron energy levels in this region form a continuum and a continuous absorption spectra would be expected in certain temperature ranges. Dekker (11) says this should be the case around 10^{19} donor/cc or 10^{19} impurity atoms per cubic centimeter. As the temperature is increased further, the Fermi level tends to the center of the energy gap and the energy gap effects should again be observed (32).

Much more detailed studies of semiconductors are available. Dekker (11) is suggested as a place to begin a study in

greater detail. On the basis of the band model for silicon and silicon alloys the following experiment was set up to determine the effects of boron and phosphorus on some optical properties of these doped systems.

IV. EXPERIMENTAL PROCEDURE

A. Experimental Properties Measured and Equipment

The properties measured in this study were the diffuse and the total reflectances and the transmission. These properties were measured as a function of the boron and phosphorous atomic concentrations in single crystal silicon. A variable monochromatic light source was used to provide the electromagnetic energy for the experiment.

Diffusely reflected electromagnetic energy is the energy reflected into the hemisphere above the point of incidence. This reflected energy does not include the directly reflected component. The directly reflected component is the energy which is reflected in such a way that the angle of incidence equals the angle of reflection (see Figure 7).

The sum of the diffusely reflected energy and the specularly reflected energy equals the total reflected energy. This total reflected energy was one of the quantities measured in this study. The specularly reflected energy was calculated as the difference between the total and the diffusely reflected energy. The energy transmitted through the specimen was measured for the transmission data.

Measurement of the total and diffusely reflected quantities was accomplished using an integrating sphere along with a dual beam spectrophotometer. The integrating sphere was a 6-inch hollow sphere cut from an aluminum block and coated on

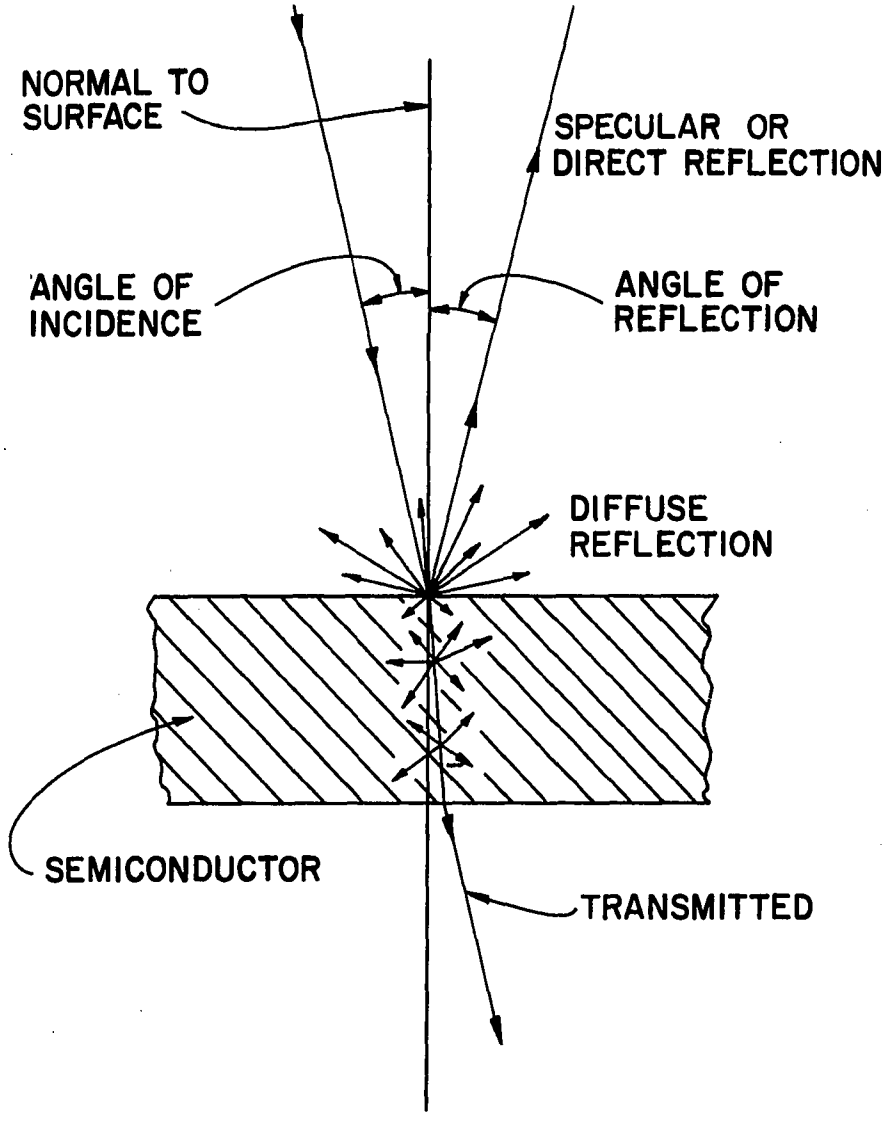

Figure 7. Schematic representation of electromagnetic interaction with a semiconductor

the inside with magnesium oxide. The sphere was formed in two halves with two 0.75-inch holes in one-half of the sphere for the reference beam and the sample beam to enter the sphere. The other half was provided with mounting positions for the specimen and a reference surface. The specimen position was directly across the sphere from the specimen beam port. The reference surface was directly across the sphere from the reference beam port. See Figure 8 for a pictorial diagram showing the light paths and the general layout of the integrating sphere. The energy recording transducer used in this experiment was a lead-sulfide detector.

The reference surface was a magnesium oxide wafer on an aluminum backing plate. The magnesium oxide was deposited on the aluminum plate and on the inside of the hollow sphere by burning magnesium strips and allowing the smoke to condense on the surfaces. This process is described in a U.S. Bureau of Standards bulletin as a "fine grained, diffusing surface of high reflectance" (41). A freshly prepared surface has a reflectance of about 0.96-0.98 over the wavelength range used in this study (5).

This dual beam arrangement of the monochromatic light source measures the ratio of the energy reflected from the specimen to the energy reflected from the reference. Using the dual beam, the energy intensities directed to the specimen and the reference surface are the same. Therefore, by defining the reflectance of a surface as the ratio of the reflected

1. *oscillating mirror*
2. *sample beam mirror*
3. *reference beam mirror*
4. *integrating sphere*
5. *entrance ports (cells are placed here for absorbance and transmittance measurements)*
6. *exit ports (sample and reference materials are placed here for reflectance and fluorescence measurements; otherwise, ports are normally covered with magnesium oxide plates)*
7. *integrating sphere opening (filter is placed here for fluorescence measurements)*
8. *detector*

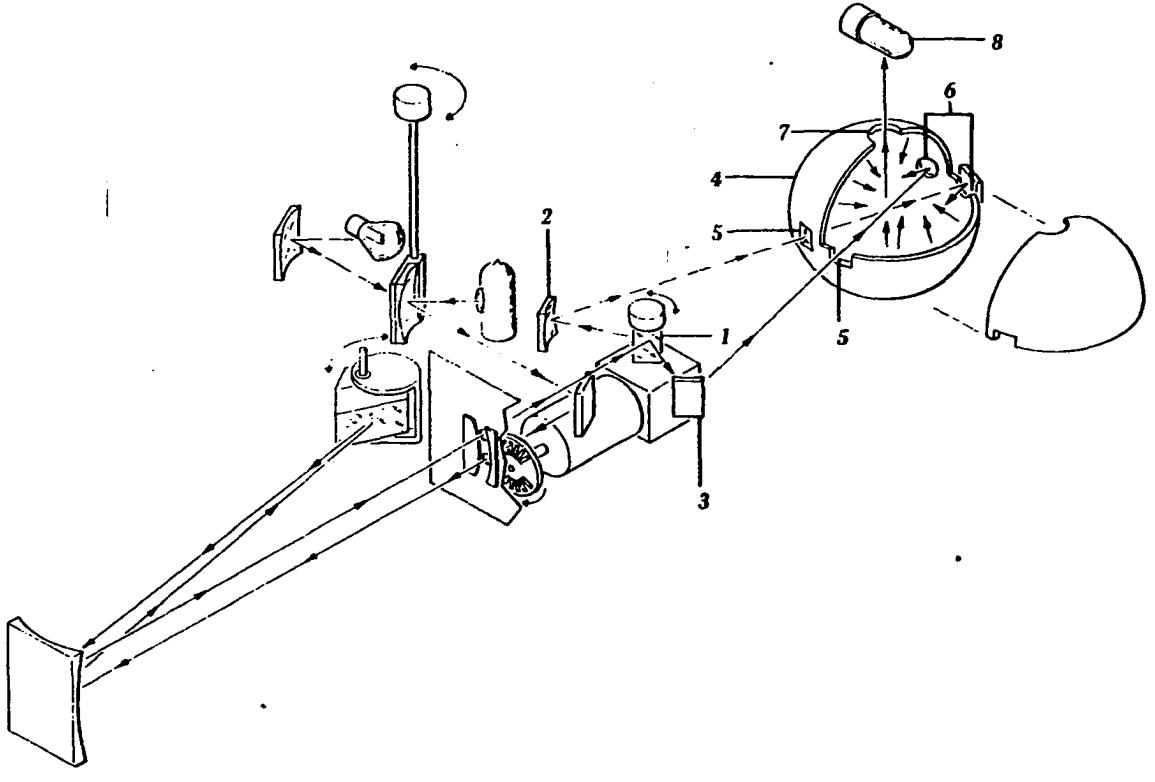

Figure 8. Cutaway view of monochromator and integrating sphere (40)

energy to the incident energy, one can set up a ratio as follows

$$r_{ref} = \frac{E_{ref}}{E_o} \quad , \quad r_{sam} = \frac{E_{sam}}{E_o}$$

$$\frac{r_{sam}}{r_{ref}} = \frac{E_{sam}}{E_{ref}} \qquad [22]$$

E_{ref} - Energy reflected from the standard surface

E_{sam} - Energy reflected from the specimen

E_o - Energy incident on the specimen and on the standard surface

r - Reflectance of the surface

Knowing the reflectance of magnesium oxide, the reflectance of a sample can be found since the integrating sphere with its lead-sulfide detector measures the ratio of the energy reflected from the sample to the energy reflected from the reference surface. Using this technique the reflectances were measured as a function of the wavelength from 0.550 microns (10^{-6} meters) to 2.2 microns.

Two types of reflectances were measured, the diffuse and the total, see Figure 7. To accomplish these measurements the position of the specimen surface with respect to the incident beam was controlled. Since the reference surface was magnesium oxide, its position did not have to be changed due to the diffuseness of its reflected energy. This was tested

and found to be true by trial in both positions. To measure the diffusely reflected energy the specimen was positioned so that the angle of incidence was zero. Thus, the specularly reflected component of the reflected energy was directed back out the port through which it entered the sphere. The reflected energy measured by the detector was then the diffusely reflected portion. Measurement of the total reflected energy was accomplished by directing the directly reflected or specularly reflected component away from the beam port so that its energy would also be collected. Taking the difference between the total reflectance ratio and the diffuse reflectance ratio gives the specular reflectance ratio. Then knowing the reflectance of magnesium oxide the various quantities can be calculated.

The transmitted energy was also measured using the integrating sphere and the dual beam spectrophotometer. To accomplish this measurement the sample and reference ports for reflectance were covered with magnesium oxide wafers. The sample to be measured was placed in the beam directed at the sample position but ahead of the integrating sphere, Figure 8. The other beam was left free of obstructions. Then the lead-sulfide cell received the signal from the energy transmitted through the specimen and from the incident beam itself. The ratio of these signals was recorded.

The dual beam monochromatic light source was a Beckman DK-2A unit which provides the output as a plot of the detector

signal ratios versus the wavelength using an X-Y plotter. A sample of this data appears in the Appendix. The reflectance attachment was Beckman model 24500. A photograph of this equipment appears in Figure 9.

B. Specimens

The purpose of this study was to investigate the effects of minute amounts of selected impurities in a semiconductor on its optical properties. It was decided to use silicon since some of its optical and electrical properties are available in the literature. Two detailed papers (32 and 13) report experimental results for silicon doped with phosphorus and boron. On this basis it was decided to use boron and phosphorus doping and to extend the range of doping concentrations beyond those examined by Fan and Becker (13). The wavelength range was also extended to lower limits than those reported by Fan and Becker.

Single crystals of silicon were purchased from a commercial supplier. Each sample was rough cut and machined to a 0.75-inch diameter by 0.75-inch long. The various concentrations of boron and phosphorous were supplied as ordered. Phosphorus produced an n-type crystal while boron produced a p-type crystal. The doped single crystals and the intrinsic crystal were produced by the Czochralski method (2). Table 1 gives the information as to type of specimens used.

Figure 9. Photograph of monochromator and reflectance attachment (40)

Figure 10. Photograph of a specimen

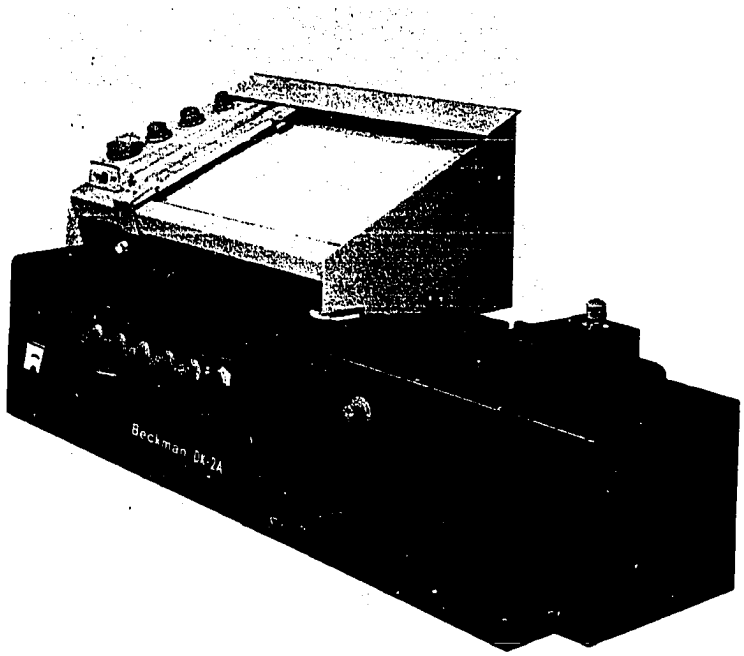

Figure 9. Photograph of monochromator and reflectance attachment (40)

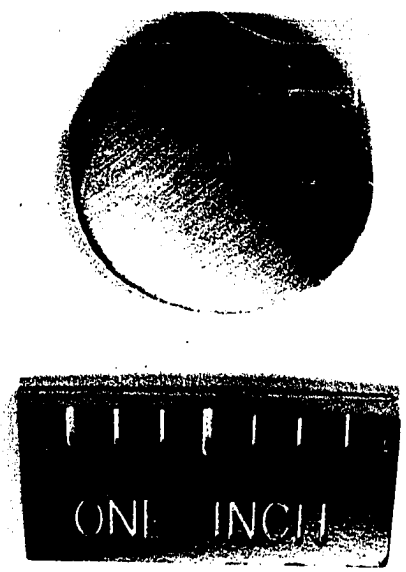

Figure 10. Photograph of a specimen

Table 1. Experimental single crystal specimens

Samples[a]	Doping atoms/cubic centimeter	Type of doping	Thickness inches
Intrinsic[b]	none	--	0.964
1	$8x10^{15}$	Boron	0.626
2	$1x10^{18}$	Boron	0.672
3	$1x10^{20}$	Boron	0.922
4	$1x10^{22}$	Boron	0.062
A	$1x10^{14}$	Phosphorus	0.724
B	$1x10^{16}$	Phosphorus	0.573
C	$1x10^{18}$	Phosphorus	0.655
D	$1x10^{20}$	Phosphorus	0.817
E	$1x10^{18}$	Phosphorus	0.066

[a]All specimens were at least 0.75 inches in diameter.

[b]This crystal had a tested resistivity of 20,000 ohm/cm.

The single crystal was used to reduce the influence of grain boundaries and other crystal discontinuities on the reflective and other properties. Due to the method of production the effect of the grain boundries and discontinuities were assumed the same for all specimens.

C. Specimen Preparation and Surface Finishes

The diffuse and specular reflectance of electromagnetic radiation in the visible and near infrared region is greatly

affected by changes in surface finish (4). Every effort was made to produce surface finishes which could be reproduced. Other preparation consisted mainly in temperature control and care of the specimens. Each specimen was individually stored and polished to avoid contamination from impurities from the other specimens or from the atmosphere.

The final polishing process consisted of mechanically polishing the specimens on carborundum wet sandpaper with a 600 grit size. This produced a satin-like finish which was readily reproduced as indicated by the fact that the specular reflectance was nearly the same for all specimens. The specular reflectance is almost entirely a function of surface finish (3). Each specimen had its own sandpaper to avoid contamination by impurities from the other crystals. This was necessary due to the very low concentrations in some specimens and the great range of atomic concentrations used. After polishing each specimen was washed with acetone to remove any grease or foreign matter and was wrapped in a piece of tissue paper. Each specimen was stored in a plastic bag to seal out the atmosphere.

Some of the specimens used in the transmission studies were cut to about 0.8 millimeter using a corborundum cutoff wheel. Each side of these specimens was finished using the 600 grit water sand paper. These specimens were mounted on a carboard mount for handling with a hole cut in the cardboard to allow the radiation to pass. A picture of one of these

mounted specimens appears in Figure 10. For the specimens with higher transmission, such as the intrinsic, larger thicknesses were used. Both surfaces of each of these specimens were also polished as above.

D. Discussion of the Experimental Procedure

The reflectivity is measured relative to a reference mirror of magnesium oxide. Such measurements may be made with a high precision, but the accuracy is often questionable since it depends on the accuracy with which the reflectance of the reference mirror is known at the time the reflectance of the specimen is measured. In an effort to reduce this variation to a minimum, standards were prepared each time tests were run and were allowed to age about one day before use. In this way the changes in reflectance with time could be reduced greatly (35) and the usual accumulation of dust from the air with time could be nearly eliminated.

The area of the specimen which is illuminated varies slightly with wavelength due to the automatic control of the light slit width to maintain operation of the detector at peak sensitivity. This may cause an error if the specimen is not sufficiently homogeneous. Single crystals of the specimens were used in an effort to provide a homogeneous surface material. The surface finish across the specimen was the other variable for a homogeneous specimen. Careful preparation of the specimen produced a surface which appeared very

homogeneous when studied under a microscope. With the 600 grit water polishing procedure this problem probably was of little importance.

With any device using radiant energy there is danger of radiation other than that being measured, falling on the specimen due to scattering in the monochromator. Tests for this would be difficult to make. The following procedure was used to determine if there were any large effects due to this problem. Both the reference and the specimen parts of the reflectance unit (see Figure 8) were covered with magnesium oxide wafers prepared by the same procedure. A reflectance ratio test was run. Then the two wafers were exchanged and the reflectance ratio test run again. Any large differences observed would indicate a difference in the illumination or in reference finish. No significant differences were noted using this test on the Beckman monochromator and reflectance attachment used for this study.

Light scattered from the specimen or reference can escape through the entrance ports of the integrating sphere. These effects should tend to balance out due to the nature of the operation of the integrating sphere. In a ratio recording mode of operation this effect should be of little importance. However, if the total reflected energy were being observed, McKeehan and others (27a) have calculated a correction factor to account for these losses. The present study used the ratio recording mode of operation for all data.

V. EXPERIMENTAL RESULTS AND CALCULATIONS

Using the Beckman ratio recording spectrophotometer, the spectral diffuse reflectance was measured for the specimens listed in Table 1. A magnesium oxide wafer was used as the reference for these measurements. Using equation 22 and spectral reflectance data from Middleton (27b) and Sanders (35) for the absolute reflectance of magnesium oxide (see Appendix), the diffuse and total reflectances were calculated as a function of energy. These results are presented in Figures 11 through 19.

The diffuse reflectance curves were used to determine the absorption edge using the method proposed by Fochs (14). These curves in Figures 11, 12, 16 and 17 show a definite decrease in diffuse reflectance as the photon energy increases. This decrease has a definite linear region of greatest slope which is attributed to an exponential rise in the absorption coefficient. According to Fochs, the onset of this straight line portion of the diffuse reflectance as the energy decreases provides a means of determining the absorption edge. This position is indicated by the short vertical dotted line extending downward at the end of the straight line portion of the reflectance curve. The values of the edge determined in this manner are tabulated in Table 2.

The total reflectance curves are plotted on the same figure with the diffuse reflectance. Some experimental values

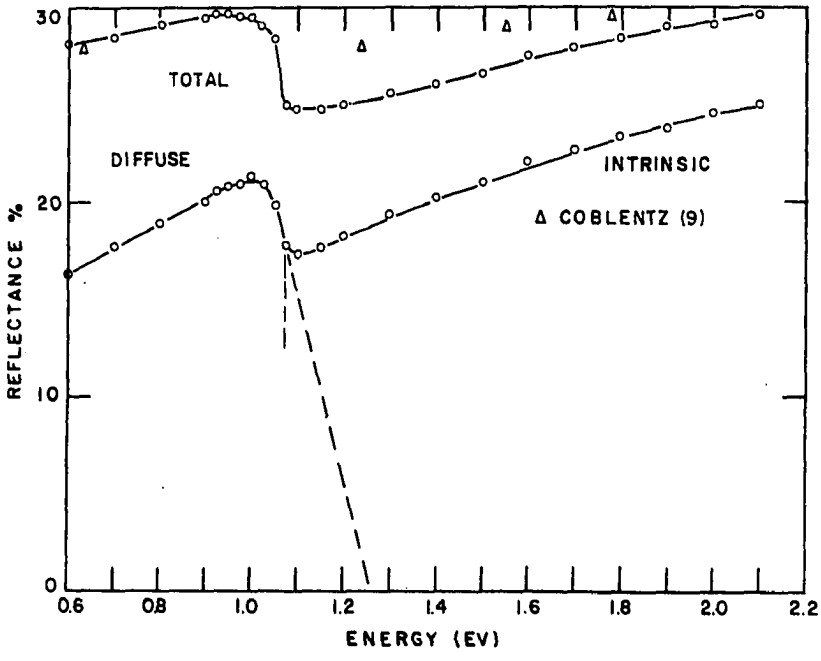

Figure 11. Reflectance versus energy

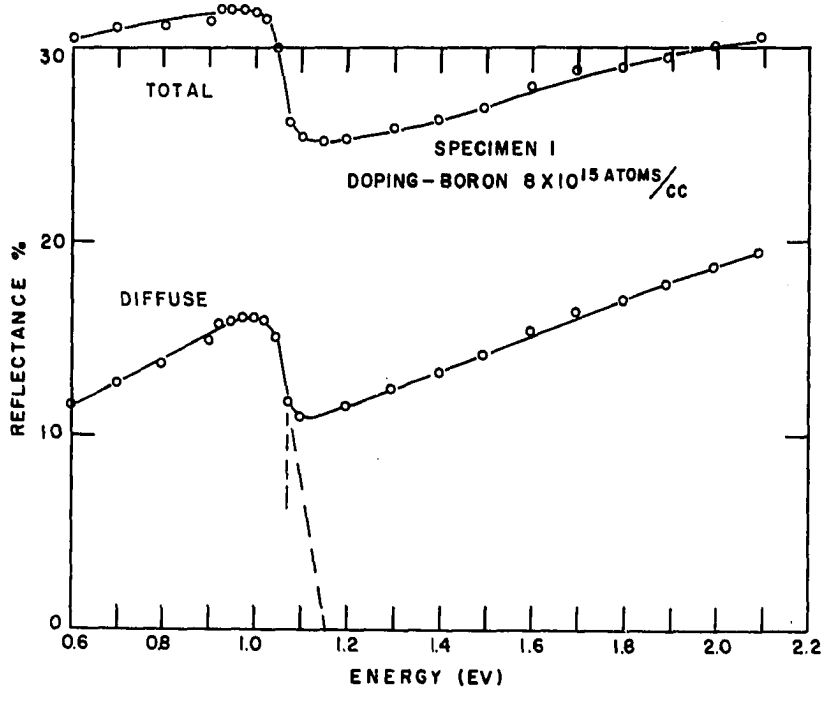

Figure 12. Reflectance versus energy

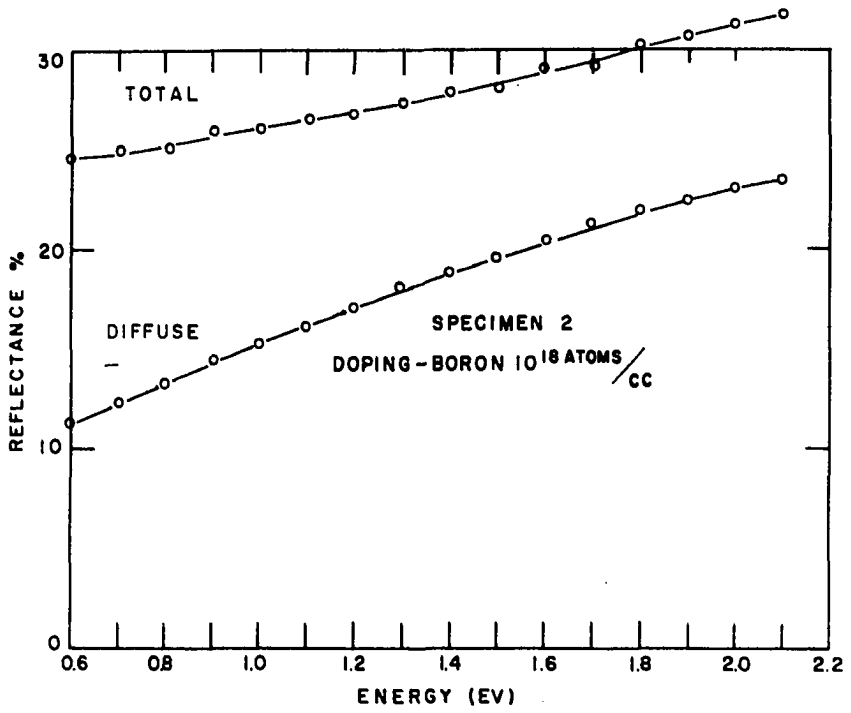

Figure 13. Reflectance versus energy

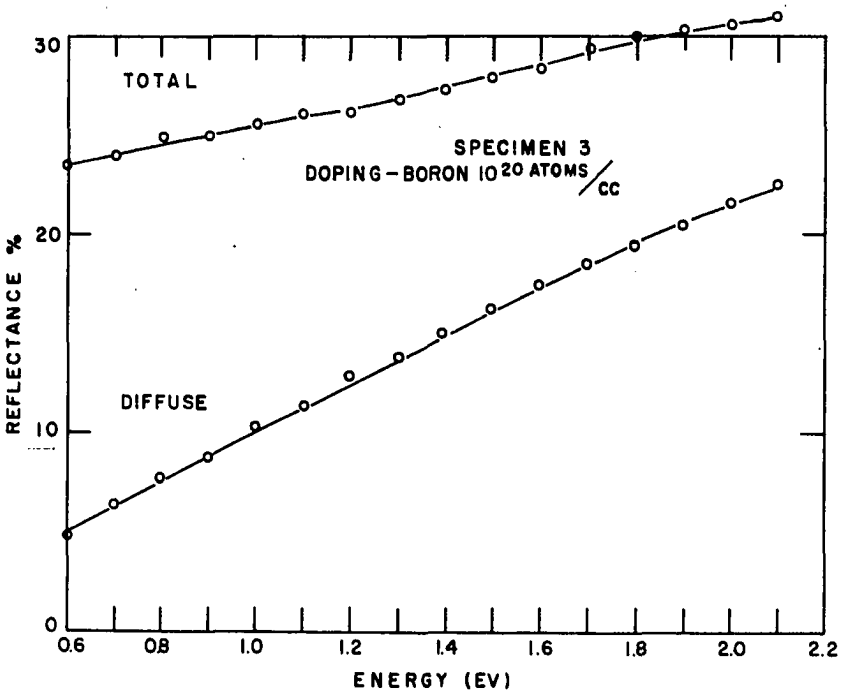

Figure 14. Reflectance versus energy

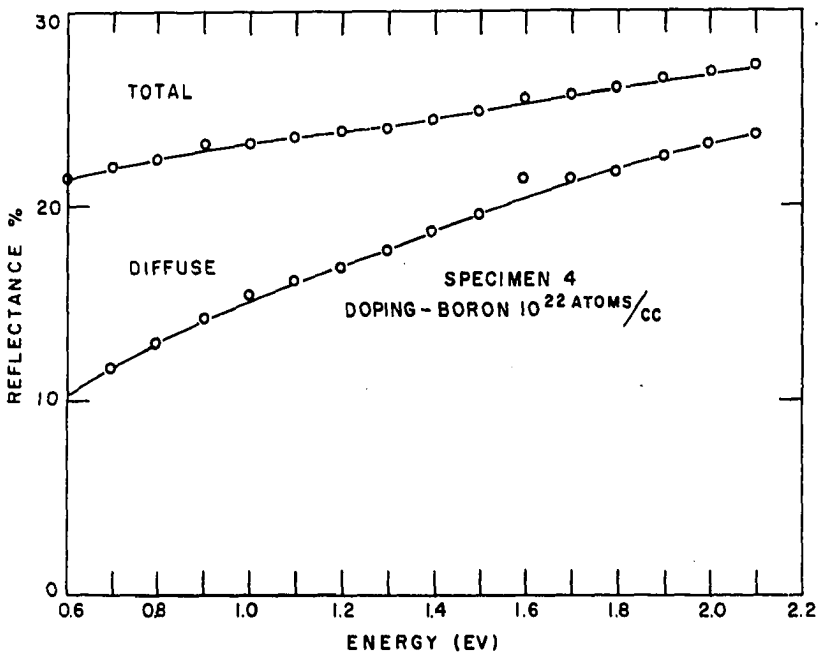

Figure 15. Reflectance versus energy

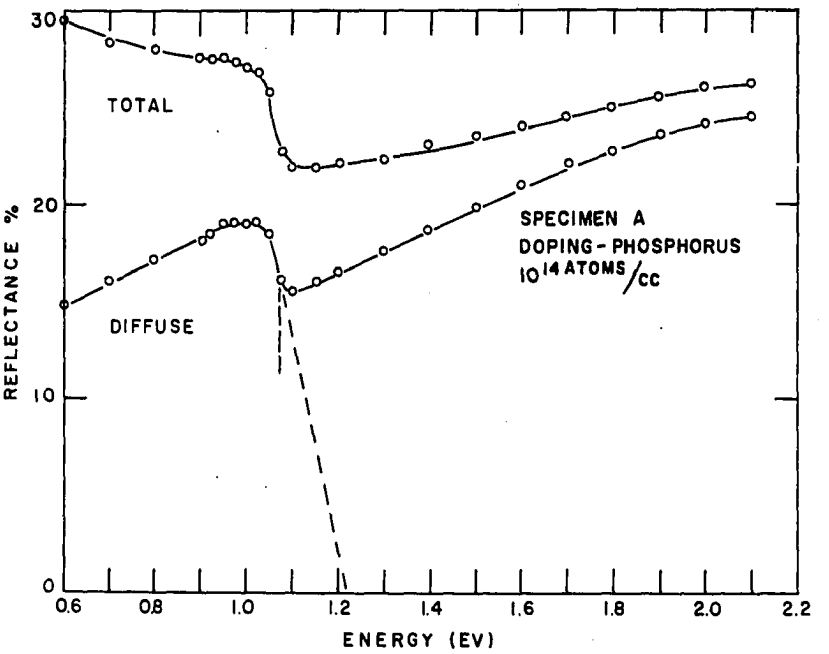

Figure 16. Reflectance versus energy

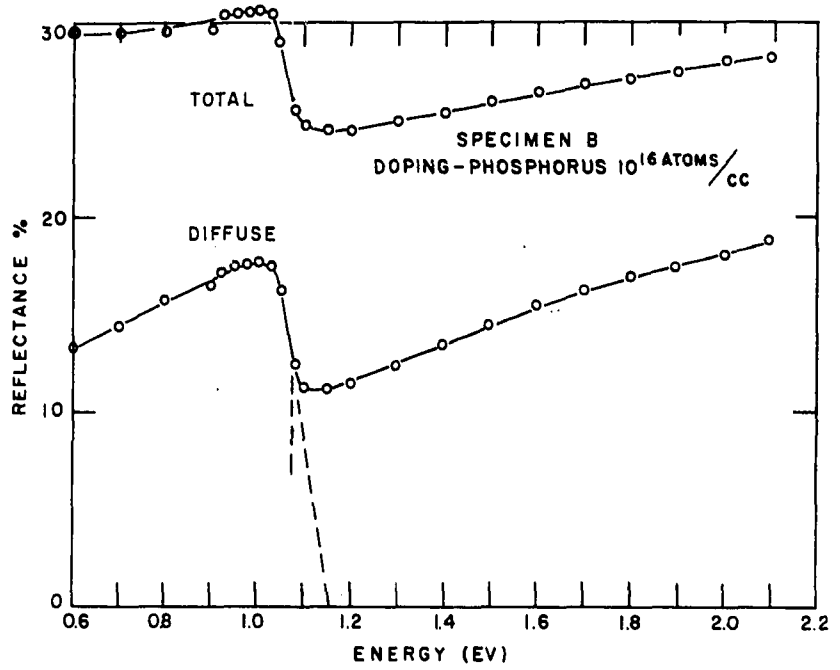

Figure 17. Reflectance versus energy

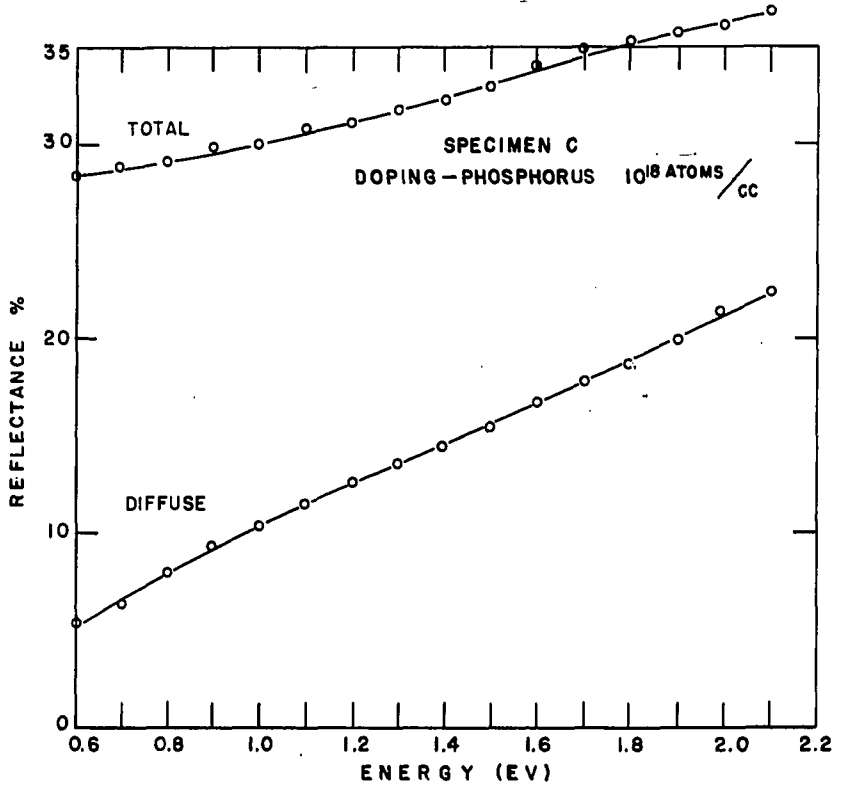

Figure 18. Reflectance versus energy

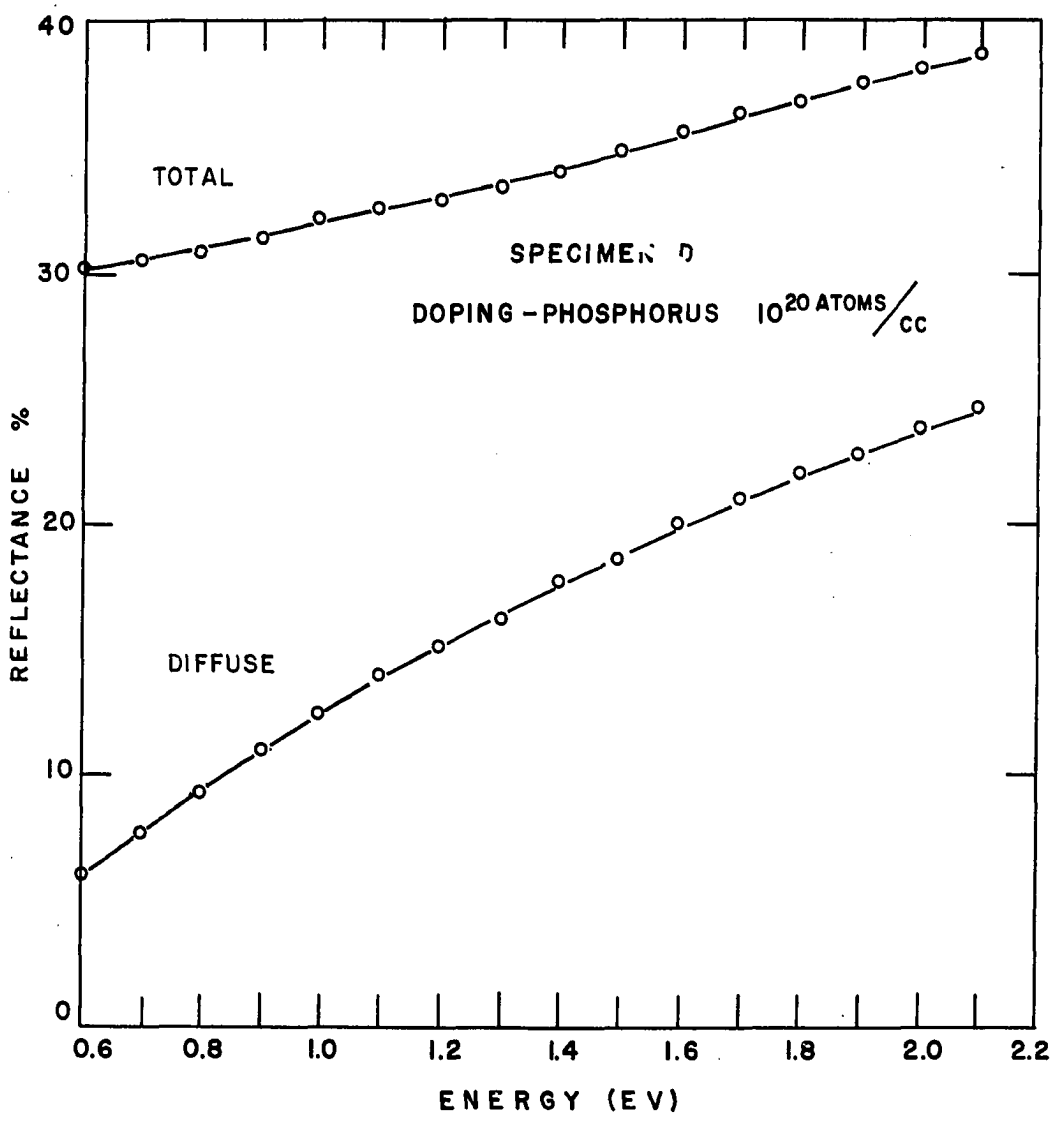

Figure 19. Reflectance versus energy

Table 2. Experimental room temperature activation energy

Specimen	Method	
	Diffuse reflectance	Absorption coefficient
	Absorption edge (ev)	Absorption edge (ev)
Intrinsic	1.07	1.04
A	1.08	1.04
B	1.08	1.05
D		1.06
1	1.08	1.05

of reflectance from silicon from the literature (9) are recorded in Figure 11. These values are for comparative purposes and the relative impurity levels are unknown.

The absorption coefficient was calculated from the transmission and total reflectance data. These results are presented in Figures 20 through 24 as a function of photon energy.

Examination of these figures shows that for each of the specimens the absorption coefficient rose sharply as the photon energy approached 1.1 electron volts. This region of greatest slope shows an almost straight line increase in the absorption coefficient. This line is extended to cut the energy axis to evaluate the absorption edge (26a). The values

of energy obtained by this method are tabulated in Table 2 for comparison with the values from the diffuse reflectance curves.

Some experimental values of the absorption coefficient from the literature (13 and 32) are presented in Figures 23 and 24. The data in Figure 23 is for a boron doped specimen with about the same number of carriers as the phosphorus doped specimen D. This is intended to compare the effects of electrons and holes. The data in Figure 24 is for a specimen of similar doping and carrier concentration.

The index of refraction was calculated as a function of energy since some comparitive data for the index of refraction was available in the literature. The following equation, [1], which relates reflectance, index of refraction and index of absorption, was simplified and used to calculate the index of refraction.

$$r = \frac{(n-1)^2 + \kappa^2}{(n+1)^2 + \kappa^2} \qquad [23]$$

n - Index of refraction

κ - Index of absorption

r - Total reflectance

This equation can be simplified for this study since κ was very small compared to $(n-1)^2$ for all cases tested. The reflectance can then be written as

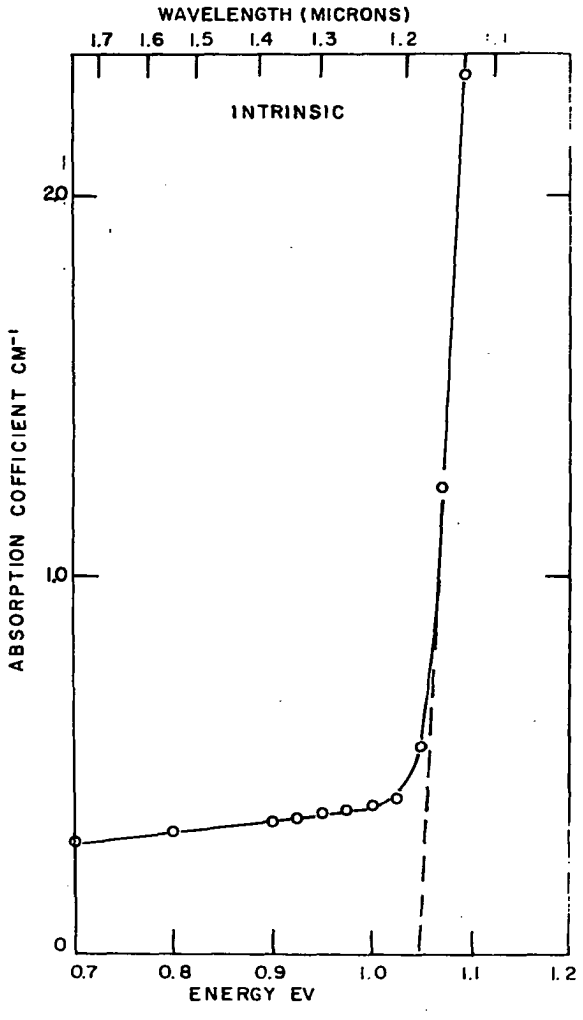

Figure 20. Absorption coefficient versus energy

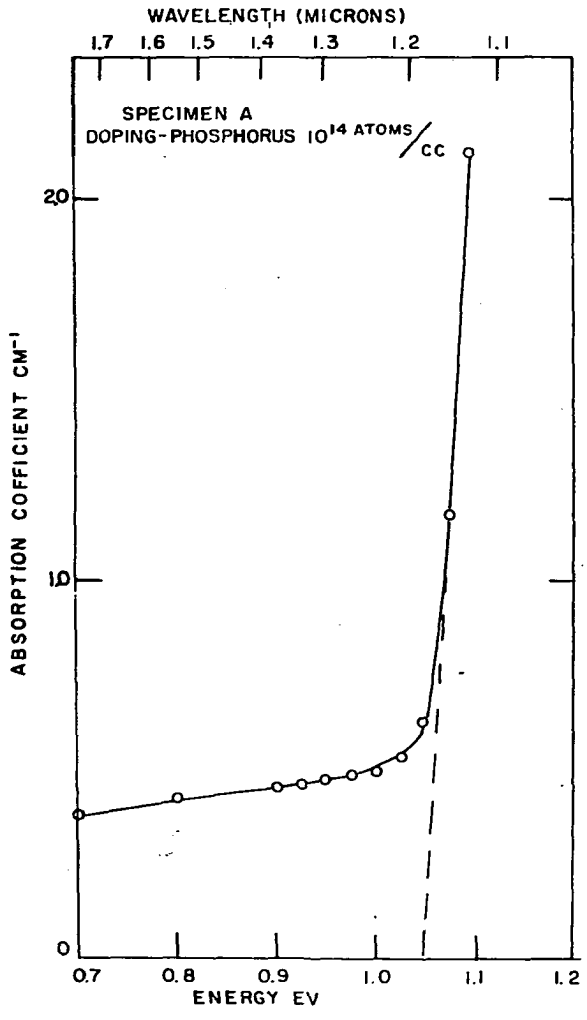

Figure 21. Absorption coefficient versus energy

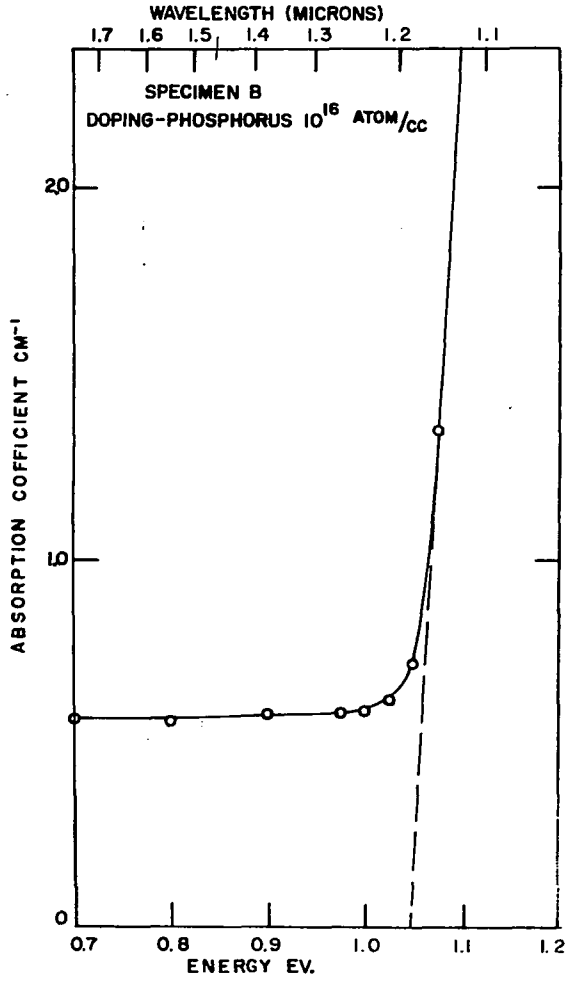

Figure 22. Absorption coefficient versus energy

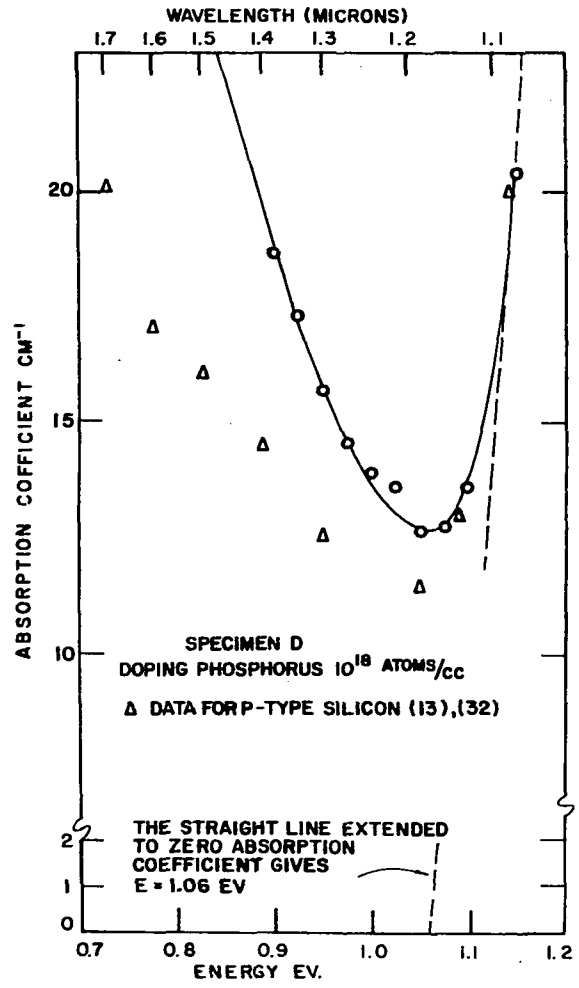

Figure 23. Absorption coefficient versus energy

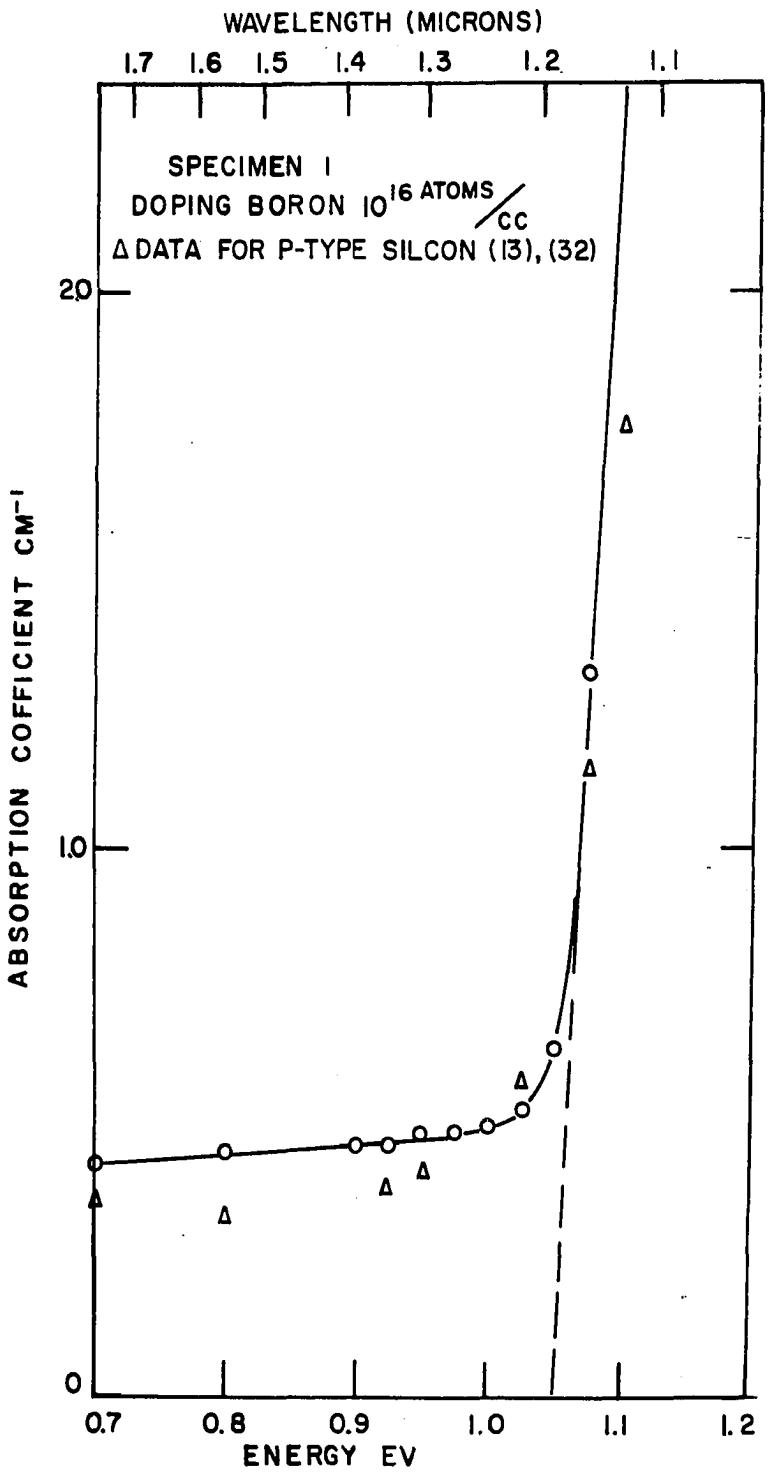

Figure 24. Absorption coefficient versus energy

$$r = \frac{(n-1)^2}{(n+1)^2} \qquad [24]$$

from which the index of refraction, n, can be calculated if r is known and if the assumption mentioned above holds. These calculated results appear in Figures 25 through 28. The curves end near the photon energy 1.1 electron volts since beyond this value the index of absorption can no longer be assumed small with respect to $(n-1)^2$ in equation 23 This is due to a rapid increase in the absorption coefficient, see equation 10

Briggs measured the values of the index of refraction using a prism made of silicon with a 99.8 percent purity. Some of his data appears in Figure 25 for comparative purposes. Using Briggs' data, we calculated the reflectance at 0.8 electron volts and obtained a value of 30.6 percent compared to our measured value of 30.2 percent reflectance for the intrinsic specimen, Figure 11.

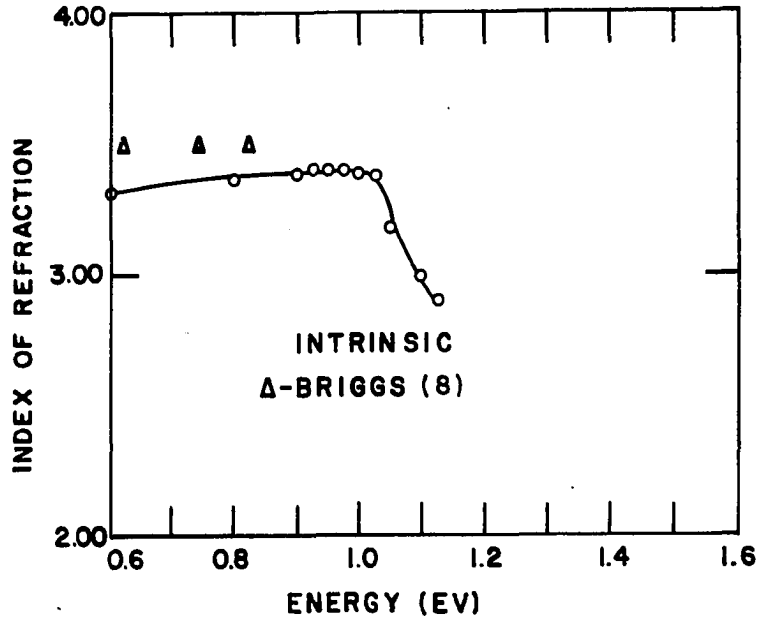

Figure 25. Index of refraction versus energy

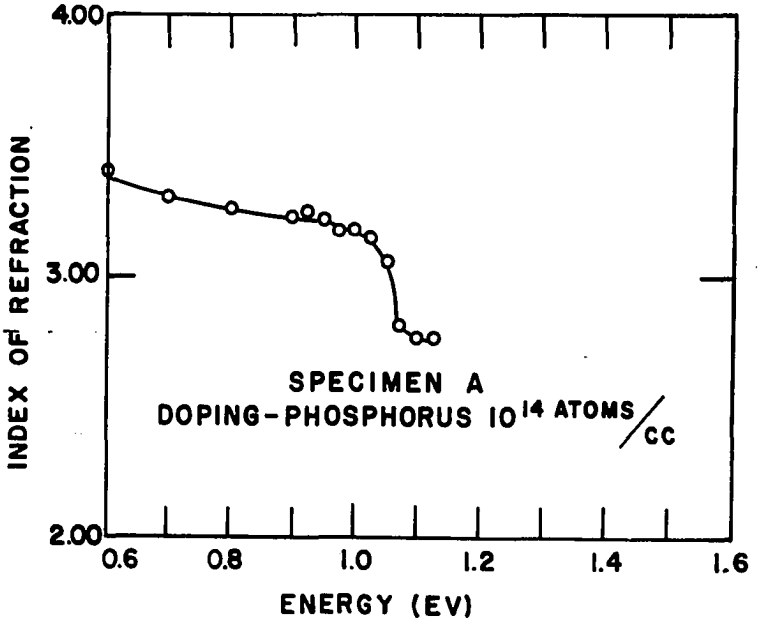

Figure 26. Index of refraction versus energy

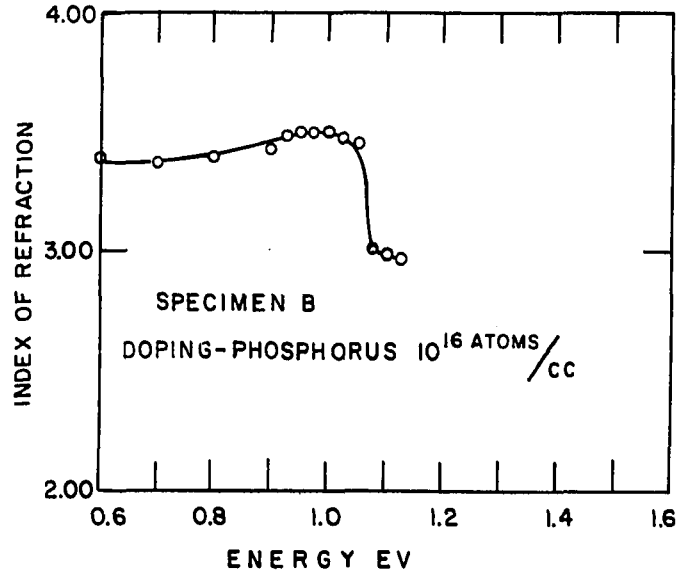

Figure 27. Index of refraction versus energy

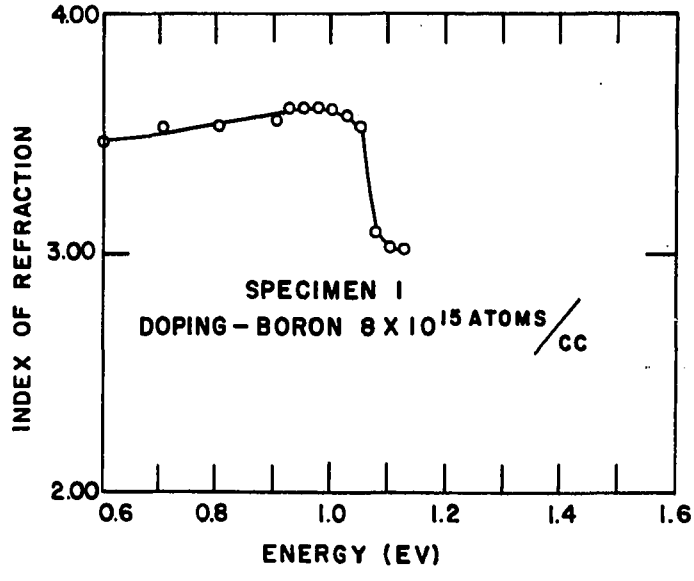

Figure 28. Index of refraction versus energy

VI. DISCUSSION AND CONCLUSIONS

Before discussing the results it should be pointed out that the main aim of this investigation is to determine the effects of specific impurities on the reflectance of silicon using an experimental technique outlined by Fochs (14). Fochs suggested that the rapid rise of the absorption coefficient with energy near an absorption edge for a semiconductor such as silicon could be applied to the interpretation of the diffuse reflectance spectrum. This rise in the absorption coefficient corresponds to an abrupt decrease in the reflectance which could be used to determine the absorption edge.

The total reflectance and the transmittance measurements were also made for the reasons given below. The total reflectance measurement provided the information for calculating the index of refraction which could be directly compared with values from the literature obtained by Briggs (8). The transmittance measurements were made to calculate the absorption coefficient because this method is often used in the literature and is widely accepted as a means of evaluating the absorption edge (13).

Let us examine the data on diffuse reflectance of the specimens. The intrinsic and the other specimens with doping concentrations of less than 10^{18} atoms per cubic centimeter of either phosphorus or boron show a substantial decrease in reflectance as the photon energy is increased above 1.0

electron volt. This region above 1.0 electron volt is the same region in which there is a sharp rise in the slope of the absorption coefficient curve, Figure 20 for example. Using Fochs' technique, the absorption edge is evaluated for each of the specimens displaying the abrupt decrease in the diffuse reflectance curves, see Table 2. An examination of the results for specimens A, B, 1 and the intrinsic specimen show that the impurity levels up to and including 10^{16} atoms per cubic centimeter do not appreciably change the value of the absorption edge.

The values of absorption edge evaluated by using Fochs' method compare quite well with the values reported in the literature. The agreement is quite remarkable, see Table 3, but Fochs (14) reports a value of 1.2 electron volts. This value for the absorption edge is higher than the accepted value.

Table 3. Activation energy of silicon at room temperature (29)

Observer	Absorption edge (ev)
Macfarlane and Roberts	1.08
Dash and Newman	1.06
Fan, Shephard and Spitzer	1.05
Bell Telephone Laboratories	1.090

Examination of experimental data reported by Fochs indicates that the maximum value of his reflectance is 60 percent. Our maximum values of reflectance were about 30 percent which agree with values reported by Coblentz (9) and others (5) for bulk silicon. Our early data from bulk samples indicated the same high reflectances of about 60 percent in this region until we discovered that the mounting aluminum button on the back of the specimen was reflecting energy back into the sphere to be recorded. After correcting for this error the total reflectance for the intrinsic specimen compared quite well with values reported in the literature for silicon, see Figure 11. It seems quite possible that the abnormally high reflectance observed by Fochs is the result of an error similar to our experience. This may be one of the reasons for his high value of 1.2 electron volts for the activation energy obtained by interpreting his diffuse reflectance data for silicon.

Continuing the examination of the reflectance data shows that the specimens in Figures 13, 14, 15 and 19 do not display an abrupt change in diffuse reflectance similar to the change shown for specimens with lower doping concentrations. Pearson and Bardeen (32) indicate that for specimens with these doping concentrations and at room temperature a condition of degeneracy or near degeneracy has set in. The boron doping concentration at which degeneracy sets in is about 3×10^{18} carriers per cubic centimeter and for phosphorus it is about

4.5×10^{18} carriers per cubic centimeter (32). Pearson and Bardeen (32) indicate that at room temperature nearly all the donors will be ionized so that the number of carriers available in the conduction band is approximately equal to the impurity concentration. Thus enough carriers are available to cause degenerate conditions at about 5×10^{18} atoms per cubic centimeter. The same reasoning holds for the boron doped positive charge carrier specimens except that a lower atomic concentration of boron will cause a degenerate system. The diffuse reflectance data can thus be used to indicate the onset of this degenerate condition with increasing carrier concentrations. As an example, the diffuse reflectance of specimen C, Figure 18 shows a bow in the region around 1 electron volt indicating the approach of degeneracy of the electron gas in the conduction band.

In addition to the abrupt change or no abrupt change in the diffuse reflectance data, certain other trends can be identified. Specimen 1, Figure 12, and specimen B, Figure 17, though having the same absorption edge energy, show a greater decrease in the reflectance than the lower doped specimen A or the intrinsic specimen. This indicates that the addition of these impurities does affect the absorption and reflectance but does not affect the absorption edge characteristics. In addition the effect of the specific impurities used in this study on the reflectance seems to be greater in the presence of negative charge carriers, phosphorus doped, than in the

presence of positive charge carriers due to boron doping. The abrupt change in reflectance at the absorption edge was greater for the phosphorus doped specimens, see Figures 16 and 17. Also, a general trend towards increasing reflectances as the doping increases was observed with this effect more pronounced for the phosphorus doped specimens.

In addition to the diffuse and total reflectance measurements, the transmission through the specimens was measured with the intention of calculating the absorption coefficient and thus be in a better position to evaluate the accuracy of the technique proposed by Fochs (14) and used by Wooley and Warner (43). The absorption coefficient was plotted for all specimens showing any transmission in our investigation.

Comparative data from the literature (13 and 32) for the absorption coefficient at room temperature is plotted along with our results in Figures 22, 23 and 24. This comparative data was obtained by estimating the resistivity at room temperature (32) as a function of the impurity and its concentration and using this resistivity to estimate the absorption coefficient as a function of wavelength from Fan and Becker (13).

Examination of the absorption coefficient results, Figures 20 through 24, indicates that the straight line extension of the line of greatest slope cuts the energy axis at about 1.05 electron volts, see Table 2 for more exact values. This energy may be taken as an estimate of the absorption

edge (26a). Comparing these results for the absorption edge with values from the literature, Table 3, a very close agrument is observed. Comparing these values with those determined using Fochs technique, see Table 2, indicates that Fochs method gives values of the absorption edge for our material which are consistently 3 to 4 percent higher, but are within the range of values reported in the literature.

To provide a further check on the data obtained from this study, the index of refraction was calculated directly from the total reflectance using equation 24. These calculated values are presented as functions of photon energy in Figures 25 through 28. Some representative data on the index of refraction from Briggs (8) is plotted in Figure 25 along with our data for comparison. Briggs used a prism of silicon to evaluate the variation of index of refraction with wavelength.

The index of refraction curves end in the region where the intense absorption sets in. In this region and at the higher energies the value of κ in equation 23 is no longer small and the index of refraction cannot be calculated using the simplified equation 24. Also, in the energy range above the absorption edge there was no transmission due to very intense absorption even in specimens less than 0.075 inches thick. Specimens thinner than this became impossible to handle because of brittleness.

To complete the discussion of the data and results of an investigation of the optical properties of silicon the effects

one might expect because of the energy band structure of this material could be reviewed, see Figure 4 or Figure 29 in the Appendix. Herman (21) indicates that there should be an appreciable number of carriers in the lower v_3 level at room temperature but we see no evidence from our experimental data which gives an indication of an indirect transition to the conduction band from this v_3 level. The energy band we apparently are observing is the band between the top of the valance band and the lowest point in the conduction band, see Figure 4, which requires an indirect transition along with a phonon interaction to conserve momentum. The reason we may not be able to observe other transitions from lower levels is because these levels are very close together or because transitions from the deeper levels are so few, in either case of which our equipment could not detect their effect.

We conclude this discussion by stating the following observations:

1) With proper precautions Fochs' technique gives a reasonably accurate estimation of the absorption edge.
2) Transmission measurements provide a very accurate method of determining the absorption edge but the method is tedious and often difficult to perform. Values obtained using Fochs' technique agreed remarkably well with the values determined by transmission studies in our investigation.

3) Fochs' method is very convenient and fast for estimating the optical absorption characteristics of materials, especially new compounds, and can also be used to estimate the onset of degeneracy as a function of impurity concentration or of other variables.

4) The type and concentration of the impurities affect the reflectance and absorption characteristics but do not affect the values of the absorption edge for silicon.

5) Negative charge carriers or electrons appear to be more effective in influencing optical reflectance and absorption characteristics than positive charge carriers or holes.

VII. SUGGESTIONS FOR FUTURE RESEARCH

An investigation of the effects of temperature on the optical properties using the same specimens studied in this test may provide further information on the effects of these impurities. A study of the temperature effects on the electrical properties, such as, Hall coefficient and conductivity, in conjunction with the study of the optical properties should be both interesting and informative. In such a study a thorough examination of the absorption edge at very low temperatures and at high impurity concentrations is suggested as an area for consideration.

Another area for investigation could be the evaluation of the heat transfer properties of the specimens used in this study as a function of the temperature. Relating this study to the investigation of the electrical and optical properties might provide useful information relating to the lattice and electronic thermal conductivities.

A third area of research could be the effect of the surface finish on the observation of the absorption and reemission processes. The study conducted for this thesis used specimens polished with 600 grit water sandpaper leaving a surface with a fine mesh of scratches, see Figure 10. The light scattered from such a rough surface constitutes a large part of the diffusely reflected radiation. This effect would tend to mask the effects of the absorbed and reemitted

radiation. It might, therefore, be interesting and informative to study an optically polished series of specimens. For such a specimen the percentage of scattered light in the diffusely reflected light could be greatly reduced and thus the absorption and reemission processes could be studied.

Finally, detailed studies of the optical properties at low temperatures as a function of the wavelength may provide a means to investigate the possibility of direct transitions to the conduction band. Other possible transitions between energy levels established by the impurities or present in the host material might also be studied at these low temperatures and at longer wavelengths.

BIBLIOGRAPHY

1. Andrews, C. L. Optics of the electromagnetic spectrum. Englewood Cliffs, New Jersey, Prentice Hall, Inc. 1960.

2. Azaroff, Leonid, and James J. Brophy. Electronic processes in materials. New York, N.Y., McGraw-Hill Book Co., Inc. 1963.

3. Bennett, H. E. Measurement of specular reflectance at normal incidence. In Blau, Henry and Fischer, Heinz, eds. Radiative transfer from solid materials. p. 166. New York, N.Y., The Macmillan Company. 1962.

4. Bennett, H. E. and J. O. Porteus. Relation between surface roughness and specular reflection at normal incidence. Journal of Optical Society of America 51: 123. 1961.

5. Betz, H. T. and O. H. Olson. Determination of emissivity and reflectivity data on structural materials. In Handbook of Thermophysical Properties of Solid Materials, Vol. 3. p. 164. New York, N.Y., Macmillan Company. 1961.

6. Blau, Henry and Heinz Fischer. Radiative transfer from solid materials. New York, N.Y., The Macmillan Company. 1962.

7. Brattain, W. H. and H. B. Briggs. The optical constants of germanium in the infrared and visible. Physical Review 75: 1705. 1949.

8. Briggs, H. B. Optical effects in bulk silicon and germanium. Physical Review 77: 287. 1950.

9. Coblentz, W. W. On reflectivity of silicon. U.S. National Bureau of Standards Bulletin 7: 197. 1911.

10. Dash, W. C. Distorted layers in silicon produced by grinding and polishing. Journal of Applied Physics 29: 228. 1958.

11. Dekker, Adrianus, J. Solid state physics. Englewood Cliffs, New Jersey, Prentice-Hall, Inc. 1962.

12. Drude, P. Zur elektranentheorie der metalle. Annalen du Physik 1: 566. 1900.

13. Fan, H. Y. and M. Becker. Infra-red optical properties of silicon and germanium. In Ditchburn, R. W. and Mott, N. F., eds., Semiconducting materials. p. 132. London, Butterworths Scientific Publications, Ltd. 1951.

14. Fochs, P. D. The measurement of the energy gap of semiconductors from their diffuse reflection spectra. Proceedings of the Physical Society of London 69, Part B: 70. 1956.

15. Foote, P. D. The total emissivity of platinum and the relation between total emissivity and resisivity. Journal of Washington Academy of Science 5: 1. 1915.

16. Forsythe, W. E., ed. Smithsonian physical tables. 9th ed. Washington, D.C., Smithsonian Institute. 1954.

17. Gubareff, G. G., J. E. Janssen, and R. H. Tasborg. Thermal radiation properties survey. Minneapolis, Minnesota, Honeywell Research Center. 1960.

18. Hagen E. and H. Rubens. Das reflexionsvermögen von metals und belegten glasspiegalen. Annalen der Physik 1: 352. 1900.

19. Harrison, T. R. Radiation pyrometry and its underlying principles of radiant heat transfer. New York, N.Y., John Wiley and Sons. 1960.

20. Herman, F. Calculation of the energy band structures of diamond and germanium crystals by the method of orthogonalized plane waves. Physical Review 93: 1214. 1954.

21. Herman, F. The electronic energy band structure of silicon and germanium. Proceedings of Institute of Radio Engineers 43: 1703. 1955.

22. Herman, F. Speculations on the energy band structure of Ge-Si alloys. Physical Review 95: 847. 1954.

23. Kronig, R. L. The quantum theory of dispersion in metallic conductors. Proceedings of the Royal Society of London 124: 409. 1929.

24. Lark-Horowitz, K. and K. W. Mussner. The optical properties of semiconductors. I. The reflectivity of germanium semiconductors. Physical Review 76: 1530. 1949.

25. Lorentz, H. A. Theory of electrons. Leipzig, Germany, B. G. Teubner. 1916.

26a. Macfarlane, G. G. and V. Roberts. Infrared absorption of germanium near the lattice edge. Physical Review 97: 1714. 1955.

26b. Maxwell, James Clark. Scientific Papers. London, Cambridge University Press. 1890.

27a. McKeehan, Jacquez, Huss, Dimitroff, and Kupperheim. An integrating sphere for measuring diffuse reflectance in the near infra-red. Journal of Optical Society of America 45: 781. 1955.

27b. Middleton, W. E. K. and C. L. Sanders. Reflectance of magnesium oxide. Journal of Optical Society of America 41: 419. 1951.

28. Morin, F. J. and J. P. Maita. Electrical properties of Si. Physical Review 96: 28. 1954.

29. Moss, T. S. Optical properties of semi-conductors. London, Academic Press, Inc. 1959.

30. Mott, N. F. and Zener C. The optical properties of metals. Proceedings of the Cambridge Philosophical Society 30: 249. 1934.

31. Newton, Isaac. Opticks. Edited by E. T. Whittaker. 4th ed. New York, N.Y. 1931.

32. Pearson, G. L. and J. Bardeen. Electrical properties of pure silicon and silicon alloys containing boron and phosphorus. Physical Review 75: 865. 1949.

33. Planck, M. The theory of heat radiation. New York, N.Y., Dover Publications, Inc. 1959.

34. Price, D. J. A theory of reflectivity and emissivity. Proceedings of Physical Society of London 62: 278. 1949.

35. Sanders, C. L. and E. E. Knowles. The absolute spectral diffuse reflectance of magnesium oxide in the near infrared. Journal of the Optical Society of America 43: 58. 1953.

36. Schocken, Klaus. The emission and reflection of radiation by metals. In Blau, Henry and Fischer, Heinz, eds. Radiative transfer from solid materials. p. 3. New York, N.Y., The Macmillan Company. 1962.

37. Snyder, N. W. Radiation in metals. Transactions of the American Society of Mechanical Engineers 74: 541. 1954.

38. Stern, Frank. Elementary theory of the optical properties of solids. Solid State Physics 15: 300. 1963.

39. Taylor, Lloyd William. Physics, the pioneer science. New York, N.Y., Houghton Mifflin Company. 1941.

40. Trujillo, Ernest F. Model DK-A ratio recording spectrophotometers. Fullerton, California, Beckman Instruments, Inc. 1962.

41. U.S. Bureau of Standards. Preparation and Colorimetric properties of a magnesium-oxide reflectance standard. U.S. Department of Commerce Bulletin LC-547. 1939.

42. Valasek, J. Introduction to theoretical and experimental optics. New York, N.Y., John Wiley and Sons. 1940.

43. Wooley, J. C. and J. Warner. Optical energy-gap variation in INAS-INSB alloys. Canadian Journal of Physics 42: 1879. 1964.

IX. ACKNOWLEDGMENTS

The author wishes to express his deep appreciation to Professor Abdul R. Rana who guided and directed this study. It was through his counseling and guidance that the author was able to appreciate and understand more fully the real complexities of this area of study.

Many others contributed their services and advice and the author wishes to thank each one, knowing he would miss someone if he tried to name all of them. A special word of thanks is due, however, to several people who were more directly connected to this project; Professor George K. Serovy who acted as co-chairman on the author's graduate committee and who took special pains to keep the way smooth and straight, Professor Glenn Murphy who aided this project with his counseling and financial support, Professor Henry M. Black who provided the author with the opportunity to taste the rich rewards of the academic life, and to Professor Harry Snyder who assisted the author with his time and whose laboratory was used for this project.

The author is forever indebted to his wife, Janice, for her patience and understanding during these years of study. Her example has always been a source of comfort and renewed strength.

X. APPENDIX

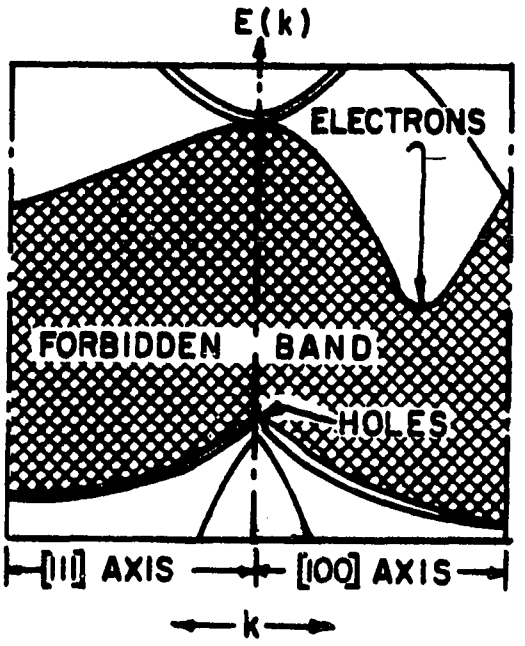

Figure 29. Schematic representation of silicon energy band structure from Herman (20) showing spin orbit interaction

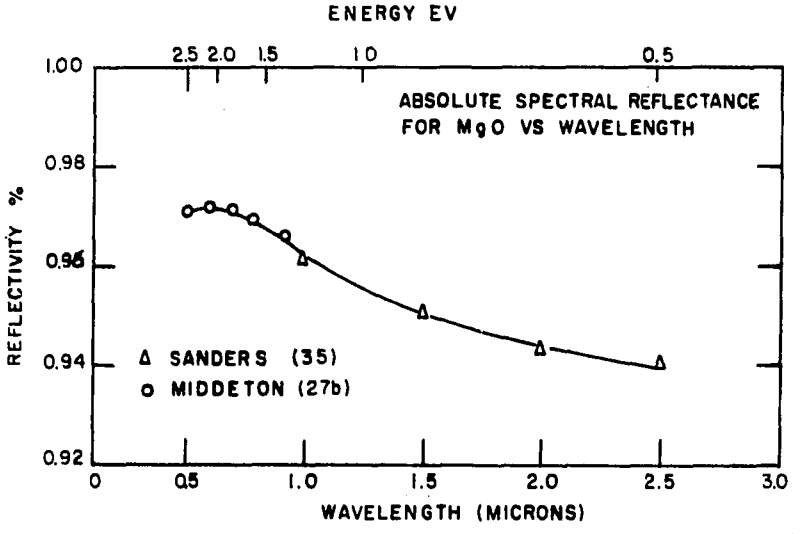

Figure 30. Absolute reflectance of magnesium oxide versus energy (27b and 35)

Figure 31. Sample Data

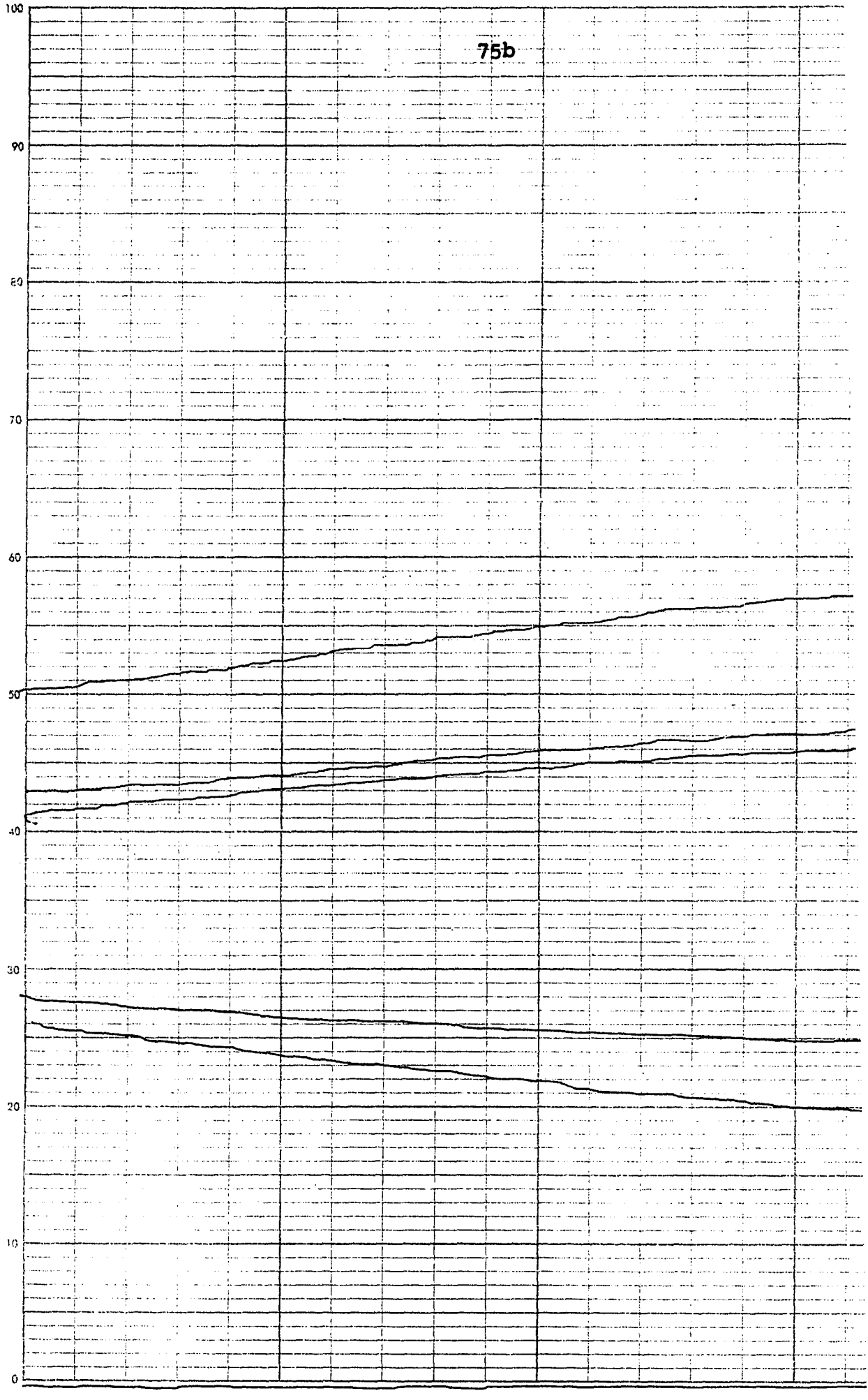
75b
100
90
80
70
60
50
40
30
20
10
0

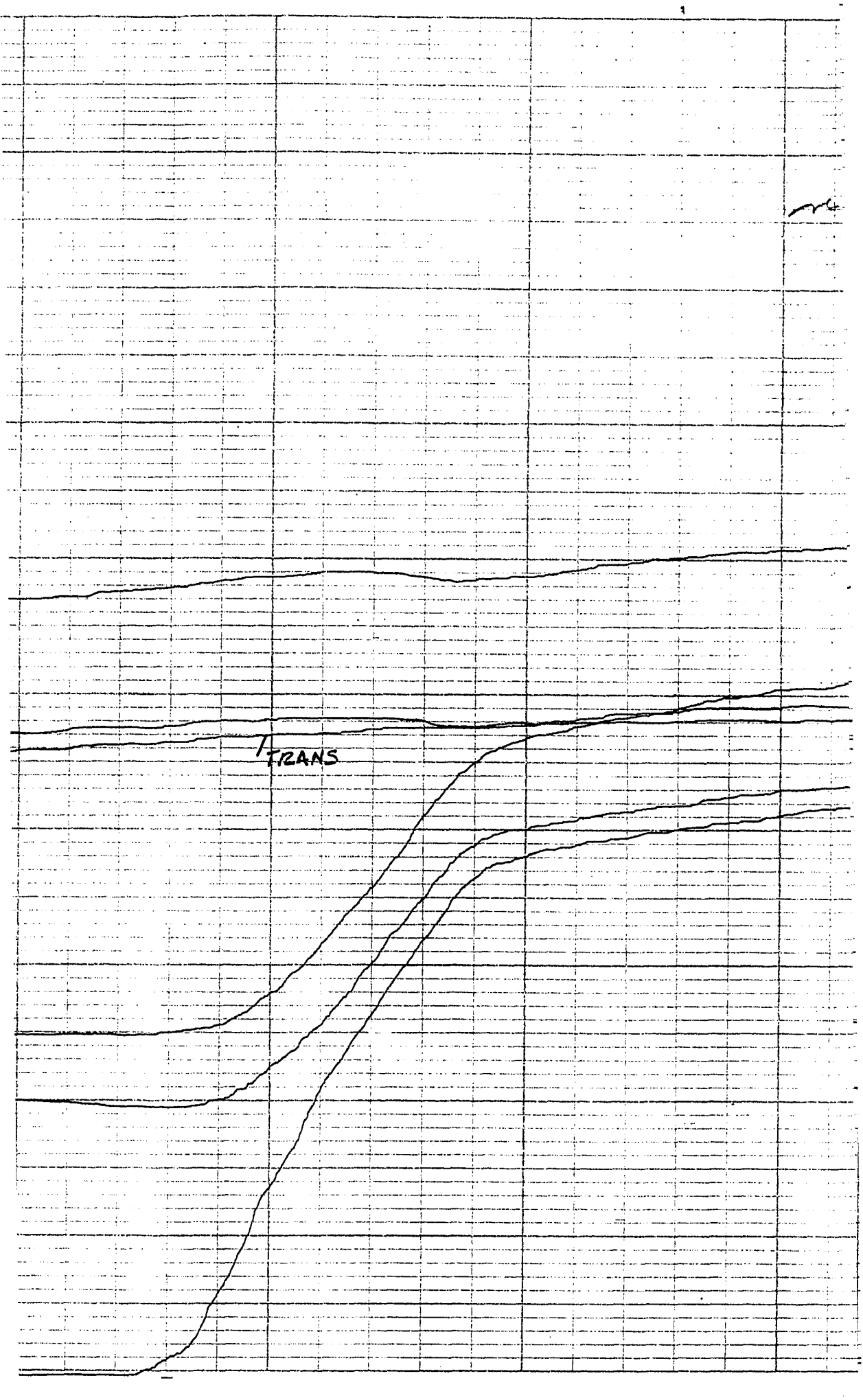
I TRANS

SPECIFY CHART NO. 12962 BECKMAN INSTRUMENTS, INC., FULLERTON, CALIF., U.S.A.